

Received November 26, 2015, accepted December 18, 2015, date of publication December 22, 2015, date of current version January 5, 2016.

Digital Object Identifier 10.1109/ACCESS.2015.2510702

Five Decades of Hierarchical Modulation and Its Benefits in Relay-Aided Networking

HUA SUN¹, CHEN DONG², SOON XIN NG³, (Senior Member, IEEE),
AND LAJOS HANZO³, (Fellow, IEEE)

¹Research Group of Communications, Signal Processing and Control, School of Electronics and Computer Science, University of Southampton, Southampton SO17 1BJ, U.K.

²University of Southampton, Southampton SO17 1BJ, U.K.

³School of Electronics and Computer Science, University of Southampton, Southampton SO17 1BJ, U.K.

Corresponding author: L. Hanzo (lh@ecs.soton.ac.uk)

This work was supported in part by the European Research Council Advanced Fellow Grant and in part by the Engineering and Physical Sciences Research Council U.K. under Grant EP/L018659/1.

ABSTRACT Hierarchical modulation (HM), which is also known as layered modulation, has been widely adopted across the telecommunication industry. Its strict backward compatibility with single-layer modems and its low complexity facilitate the seamless upgrading of wireless communication services. The specific features of HM may be conveniently exploited for improving the throughput/information-rate of the system without requiring any extra bandwidth, while its complexity may even be lower than that of the equivalent system relying on conventional modulation schemes. As a recent research trend, the potential employment of HM in the context of cooperative communications has also attracted substantial research interests. Motivated by the lower complexity and higher flexibility of HM, we provide a comprehensive survey and conclude with a range of promising future research directions. Our contribution is the conception of a new cooperative communication paradigm relying on turbo trellis-coded modulation-aided twin-layer HM-16QAM and the analytical performance investigation of a four-node cooperative communication network employing a novel opportunistic routing algorithm. The specific performance characteristics evaluated include the distribution of delay, the outage probability, the transmit power of each node, the average packet power consumption, and the system throughput. The simulation results have demonstrated that when transmitting the packets formed by layered modulated symbol streams, our opportunistic routing algorithm is capable of reducing the transmit power required for each node in the network compared with that of the system using the traditional opportunistic routing algorithm. We have also illustrated that the minimum packet power consumption of our system using our opportunistic routing algorithm is also lower than that of the system using the traditional opportunistic routing algorithm.

INDEX TERMS Hierarchical modulation, coded modulation, cooperative communication, *Ad Hoc* network, opportunistic routing.

NOMENCLATURE

AM	Amplitude Modulation	ExOR	Extremely Opportunistic Routing
AWGN	Additive White Gaussian Noise	FER	Frame Error Rate
BER	Bit Error Ratio	MIMO	Multi-Input Multi-Output
BICM	Bit-Interleaved Coded Modulation	MPEG	Moving Picture Experts Group
BS	Base Station	MRM	Multi Resolution Modulation
CDF	Cumulative Distribution Function (CDF)	MS	Mobile Station
COFDM	Coded Orthogonal Frequency Division Multiplexing	HDTV	High Density TV
CSI	Channel State Information	HM	Hierarchical Modulation
DCMC	Discrete-Input Continuous-Output Memoryless Channel	HMOR	Hierarchical Modulated Opportunistic Routing
DN	Destination Node	OR	Opportunistic Routing
DVB	Digital Video Broadcasting	PM	Phase Modulation
		PMF	Probability Mass Function
		PWC	Packet Power Consumption
		RN	Relay Node

SDTV	Standard Density TV
SN	Source Node
SNR	Signal to Noise Ratio
SPM	Superposition Modulation
TC	Turbo Coding
TCM	Turbo Coded Modulation
TR	Traditional Routing
TS	Time Slot
TTCN	Turbo Trellis-Coded Modulation
UEP	Unequal Error Protection
VANETs	Vehicular <i>Ad Hoc</i> Networks

LIST OF SYMBOLS

α	The path-loss exponent
α_k	The parameters for curve-fitting schemes
γ	The instantaneous receive signal to noise ratio ($\gamma = \tilde{h}\bar{\gamma}$)
$\bar{\gamma}$	The average receive signal to noise ratio ($\bar{\gamma} = \frac{\sum_r \kappa}{N_0 d^\alpha}$)
ζ	The number of iterations in the CM decoder
η	The block size of the CM encoder/decoder
η_k	The parameters for curve-fitting schemes
κ	A constant, which is defined to be $\kappa = \left(\frac{c}{4\pi f_c}\right)^2$
Δ	The constant for curve-fitting schemes
Φ	The average throughput of the entire system
f_c	The carrier frequency
h	The instantaneous channel fading value
k	The Boltzmann's constant, which is $k = 1.38e^{-23}$
N_r	The number of maximum retransmission attempts
N_{state}	The number of the total system states
N_t	The number of maximum transmission attempts
P	Probability
\sum_t	The transmit signal power
PWC	The average packet power consumption
R_1	The twin-layer HM-16QAM ratio.

I. INTRODUCTION

The concept of the ubiquitous Digital Video Broadcasting (DVB) standard is detailed in [1], which is one of the most widely used digital TV broadcasting standards across the globe. Although it has numerous national variants in the different countries of the world, most of them are capable of transmitting both conventional standard as well as high-density TV programmes in the so-called ultra high frequency band. Baumgartner [2, Fig. 1] illustrates the family of broadcast networks associated with the DVB standards relying on either satellite-based or terrestrial or alternatively, cable-based delivery to the home. The multimedia signals are compressed in broadcast studio, as seen in Fig. 1, which then pass through the multiplexer and are forwarded to the customer through satellite (S) networks according to the DVB-S standard, or the single frequency terrestrial (T) network based on the DVB-T standard, or alternatively, through the cable (C) based network according to the DVB-C standard. The broad family of digital television

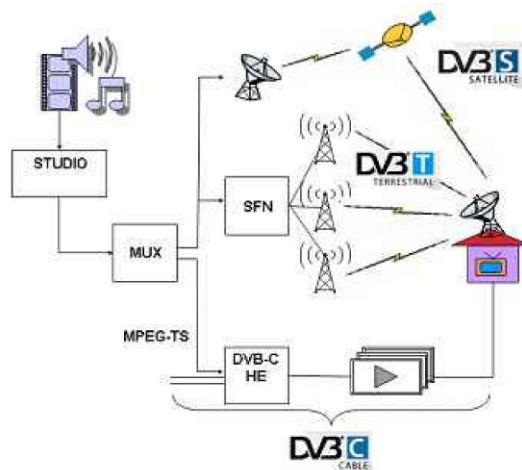


FIGURE 1. DVB-T/H based on HM © 2005 [2].

broadcast transmission techniques has been investigated for example in [1], including the Hierarchical Modulation (HM) concept.

As an integral part of the DVB standard [1], [3], HM has been widely employed in the telecommunication industry. Given the development of DVB techniques, researchers had conceived the DVB-H system for upgrading Standard Density TV (SDTV) to High Density TV, where the HM scheme was invoked for simultaneously supporting both the SDTV and HDTV services, as seen in Fig. 2 [2]. To elaborate a little further, one of the advantages of the DVB-T standard is the employment of HM schemes [2], where the SDTV signal is mapped for example to the more error-resilient pair of bits in the 4-bit/symbol 16-level Quadrature Amplitude Modulated (16QAM) scheme to ensure an adequate reception quality even in the areas, where the received signal power is low. This is facilitated with the aid of multi-level video compression, where the so-called base-layer of the video-encoded stream is mapped to the more robust pair of 16QAM bits. By contrast, the enhancement-layers of the video stream - which convey for example the higher spatial-frequency based enhancement bits required for HDTV - are mapped to the more vulnerable 2-bit ‘sub-channel’ of 16QAM.

Accordingly, observe in Fig. 2 that the non-hierarchical modulation-based HDTV system is only capable of supporting the transmission of HDTV services in the vicinity of the TV tower, but it is unable to provide more error-resilient lower-resolution SDTV services in the areas of lower received signal power. Quantitatively, in Fig. 2 a bitrate of 22.12 Mbit/s is achieved by 2/3-rate coded 64QAM for Carrier to Noise (C/N) ratios in excess of 16.5 dB. By contrast, upon employing the ubiquitous HM scheme, the HDTV services relying on both the base- and the enhancement-layer of the video stream may be supported by mapping the more important base-layer to the more robust higher priority (HP) 2-bit stream of 16QAM and the less important enhancement-layers to the lower priority (LP) 2-bit stream.

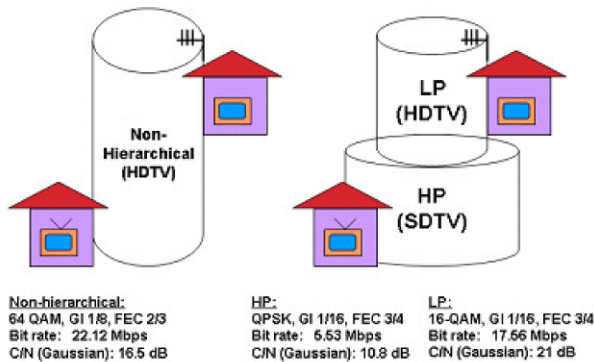


FIGURE 2. HDTV and HM © 2005 [2].

If the C/I ratio is insufficiently high for error-free receiving the more vulnerable 2-bit substream of the enhancement layer, at least the base-layer conveying SDTV is likely to be correctly received. Furthermore, the HM concept also allows the simultaneous transmission of two independent video streams over a single HM transmitter [2].

In this context the HM scheme is also eminently suitable for upgrading diverse operational telecommunication services, where new independent services may be mapped to new layers of the HM scheme, provided that the received signal power is sufficiently high. Alternatively increased-resolution HDTV services may be offered at an increased power, while maintaining a strict backwards compatibility with the legacy services relying for example on older low-resolution receivers [4], [5]. In other words, compared to a system using conventional modulation, HM has a higher flexibility, where the original and the upgraded new services are combined and broadcast to the upgraded receivers without requiring any additional bandwidth. At the same time, the original legacy devices are still supported by the upgraded broadcast system, but they are unable to receive the upgraded new services without software or hardware upgrade [6].

The attainable Bit Error Ratio (BER) performance and the achievable throughput of HM schemes have been investigated in [7] and [8], while the performance of HM schemes relying on cooperative communications had been discussed in [9] and [10]. The authors of [11]–[14] had pointed out that the layered structure of the HM scheme may also be beneficially exploited for providing Unequal Error Protection (UEP), which ensures that at least the most important multimedia information constituted for example by a low-resolution video-stream can adequately be received in the presence of a low receive Signal-to-Noise Ratio (SNR). More specifically, the authors of [3], [15], and [16] invoked a HM scheme for providing UEP for image encoding, where the information bits were mapped to specific protection layers according to their error-sensitivity based priority. Moreover, the HM scheme had also been combined with sophisticated channel coding schemes in [15]–[17] for the sake of protecting the most important information. The simulation based performance results of HM [15], [16] have

shown that receiving the information having the highest priority requires a lower received SNR (SNR_r) compared to conventional modulation schemes at a given target BER performance. However, the SNR required for flawlessly receiving the lower protection layer becomes higher than that of the identical-throughput conventional modulation scheme. Nonetheless, when considering the performance of the HM scheme in cooperative communications, the majority of research contributions documented the performance of HM schemes based on conventional constellations and the relay was assumed to be at a fixed position (often located in the middle of the source-to-destination link), which reduces both the achievable power-efficiency and the flexibility of the system.

A sophisticated relay-aided coded HM scheme was introduced in [17], where Hausl and Hagenauer combined Turbo Coding (TC) [18] with a HM scheme conceived for cooperative communications. Explicitly, the original signal sequence was broadcast by the Source Node (SN) by ensuring that the most important layer having a higher protection may be directly received by the Destination Node (DN), while the less well protected layer will be adequately received and then retransmitted by the Relay Node (RN). However, the authors of [17] only considered the specific scenario, when the position of the RN is right in the middle of the SN-DN path and invoked a specific bit-to-symbol mapping scheme. The performance of coded HM schemes was then further discussed in [19]–[22] in the context of cooperative communications, where multiple encoders were employed at the SN and all the encoded bit sequences were then superimposed layer-by-layer in order to create a HM signal sequence. Again, the less well-protected layers were assisted by the RN of the cooperative network.

The bit-to-symbol mapping optimization of the HM scheme was considered in [21] and [23]. More specifically, by appropriately designing this mapping, the HM scheme became capable of enhancing the protection of the higher-priority information at the expense of providing a weaker protection for the remaining layers. In [22], the specific position of the RN was explicitly considered in the BER analysis. For a specific coded HM, the power received at the RN should be sufficiently high for guaranteeing that the RN becomes capable of receiving the information in the lower-protection layer at an acceptable integrity. Therefore, the position of the RN explicitly influences the power allocation of the entire system. Several parameters have to be taken into consideration, when optimizing a coded HM aided cooperative communication system. On one hand, distorting the HM constellation for the sake of improving the BER of its high-priority layers at the detriment of its low-priority layers degrades its average BER, compared to conventional modulation schemes. On the other hand, sophisticated channel coding schemes, such as Trellis-Coded Modulation (TCM), Turbo Trellis-Coded Modulation (TTCM) and Bit-Interleaved Coded Modulation (BICM) [18], [24]–[27], [27]–[30] are required

for protecting each HM layer at the expense of an increased complexity. Hence, giving cognizance both to the complexity and to the power efficiency of the overall system, while maintaining its flexibility becomes a challenging task.

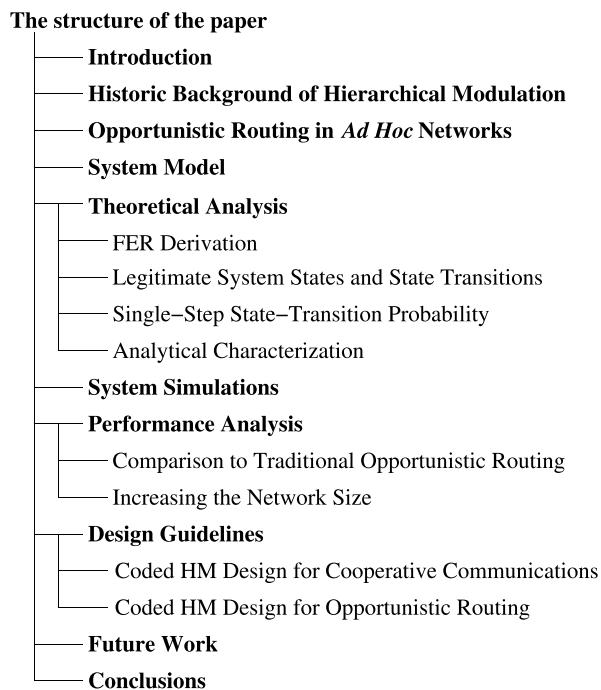


FIGURE 3. The structure of the paper.

In this paper, we provide a comprehensive survey of the HM scheme as well as of the family of opportunistic routing (OR) algorithms in the context of a wireless *ad hoc* network, leading to hitherto unpublished new coded HM schemes relying on new opportunistic relaying techniques. The organization of the paper is explicitly shown in Fig. 3: Section II outlines the historic background of the HM scheme, while Section III surveys the historic evolution of OR algorithms. Section IV introduces both our system model and our twin-layer HM-16QAM modulation scheme. The theoretical analysis of our four-node cooperative communication network is provided in Section V. Section VI characterizes our Hierarchical Modulated Opportunistic Routing (HMOR) based cooperative network, while the related performance results are illustrated in Section VII. Finally, our design guidelines are discussed in Section VIII and our future research ideas are summarized in Section IX.

II. HISTORIC BACKGROUND OF HIERARCHICAL MODULATION

The evolution and the milestones of HM schemes are portrayed in Table 1. Early in the 1960s, Lucky and Hancock published their research on the optimum performance of non-binary transmission systems [31]. Based on their pioneering work, both combined amplitude- and phase-modulation (AM-PM) as well as the quadrature amplitude modulation (QAM) had attracted substantial research

attention [32]–[35]. In 1972, Cover introduced the theory of multi-resolution transmission [32], while its applications were detailed in [33]. It had been shown that if a single source broadcasts its information to multiple receivers associated with different channel conditions, using multi-resolution transmission schemes is beneficial [34]. Based on the results of [33] and [34], in 1993, Fazel introduced the concept of on multi-resolution modulation (MRM), which was combined with multilevel coding schemes [34]. A 64-QAM constellation map of the MRM scheme was proposed in [34]. The BER versus SNR performance of a specific layer was derived, where the author illustrated that at the same SNR_r, the BER performance of the different layers is different. Additionally, Fazel also derived the performance bounds of his multi-level coding and multi-stage decoding aided schemes for transmission over both AWGN as well as Rician and Rayleigh channels.

Two years later, in 1995, Morimoto proposed HM also for satellite communications [36]. From 1995 onwards, the MRM scheme has been referred to as the HM scheme in the literature. To elaborate, Morimoto et al. [36] detailed the generation of the constellation diagram for a hierarchical 16-QAM scheme, which is considered as the typical HM constellation construction rule. Additionally [36], Morimoto et al. [37] pointed out that by distorting the HM-constellation, the overall BER performance of the HM aided system is expected to degrade, but nonetheless, the twin-layer HM-16QAM scheme employed for image transmissions was potentially capable of improving the perceived video quality due to improving the reception-quality of the visually more influential bits. As a further development, O’Leary [38] combined the HM scheme with Coded Orthogonal Frequency Division Multiplexing (COFDM) for video broadcasting, where both a non-uniform 16-QAM HM constellation as well as a non-uniform 64-QAM HM constellation were investigated. However, the investigations in [38] did not discuss the HM constellation construction rules in detail, the emphasis was on the achievable BER versus SNR performance.

The HM aided COFDM arrangement was then further investigated by Engels and Rohling in 1998 [39]. To be more specific, firstly, they proposed a triple-layer HM aided 64-DAPSK constellation, which is the first contribution that employed the HM aided DAPSK scheme instead of the classic coherently detected QAM scheme. The motivation of developing the HM aided DAPSK scheme and its construction rules was also detailed. Then, a three-mode hierarchical transmission scheme was proposed [39], where the flexibility of the HM scheme was exploited. The related HM 64-DAPSK was discussed in detail, including the corresponding bit-symbol mapping as well as the associated detection procedure. Both the BER versus SNR performance, as well as the choice of the code-rates and data rates of the different layers were illustrated.

Given the flexibility and low complexity of HM [39]–[41], it has drawn significant research interests during the

TABLE 1. Milestones in hierarchical modulation (1962-2015).

Year	Author(s)	Contribution
1962	Lucky and Hancock [32]	Investigation on N-ray system
1972	Cover [33]	Broadcasting theory
1974	Bergmans and Cover [34]	Cooperative broadcasting
1993	Fazel and Ruf [35]	Multiresolution modulation is combined with multilevel coding
1995	Morimoto <i>et al.</i> [37]	HM for satellite communication
1996	Morimoto <i>et al.</i> [38]	Hierarchical image transmission for multimedia mobile communications
1997	O'Leary [39]	HM transmission in COFDM system
1998	Engels and Rohling [40]	64-DAPSK in hierarchical COFDM system
1999	Schill <i>et al.</i> [41] Nokes and Mitchell [42]	HM for broadcasting based on multilevel codes Potential benefits of HM
2000	Seeger [43]	Coded HM for broadcast communication over fading channel
2001	Vitthaladevuni and Alouini [44]	BER computation of 4/M-QAM HM
2002	Hwang and Kim [45]	Adaptive HM for multicast communication
2003	Vitthaladevuni and Alouini [46]	BER computation of generalized HM QAM
2004	Pons <i>et al.</i> [47]	Enhanced TCM coded HM
2005	Barmada <i>et al.</i> [48] Jiang and Wilford [6]	HM QAM based H.264 video transmission HM for upgrading digital broadcasting
2006	Hossain <i>et al.</i> [7], [49], [50] Chang <i>et al.</i> [51]	Adaptive HM for multiclass data transmission Adaptive HM QAM based low-complexity H.264/AVC video transmission
2007	Hausl and Hagenauer [17]	Relay aided Turbo coded HM communication
2008	Wang and Yi [52]	Enhanced HM optimization
2009	Chang and Lee [9] Hellge <i>et al.</i> [3]	Analysis of HM aided cooperative communication over Rayleigh fading channel HM for DVB-H broadcast services
2010	Park [21]	HM aided network coding for two-way relay transmission
2011	Arslan <i>et al.</i> [15] Peng <i>et al.</i> [53]	Coded HM for progressive image transmission Hierarchical cooperative relay aided heterogeneous networks
2012	Chang <i>et al.</i> [54] Hu and Liu [55]	Optimized UEP for Multiplexed HM Low-complexity LDPC coded HM aided broadcasting system design and implementation
2013	Wang and Cai [56] Meric <i>et al.</i> [57] Mouhouche <i>et al.</i> [58]	Fair scheduling of the HM in wireless communications Adaptive CM aided HM in satcom system Throughput of HM aided precoded OFDM
2014	Saeed <i>et al.</i> [59]	Space-time coded aided HM with MRC reception in Nakagami-m channel
2015	Sun <i>et al.</i> [60]	HM aided TCM for cooperative communications

post-2000 era. In [42] Seeger conceived HM-aided coded modulation for broadcast systems. He considered a cellular environment, where the users supported by the Base Station (BS) may be divided into two groups according to their distance, namely the high-quality and low-quality regions. For the two groups defined in [42], the required receive SNRs were $\text{SNR} = 18$ dB and $\text{SNR} = 8$ dB, respectively. Then, the lower-BER base-layer and the higher-BER enhancement layer may be combined by the HM scheme, where the code rate of the two groups may be appropriately adjusted. The resultant system may guarantee that the cell-centre region is capable of receiving both the base and the enhancement layers, while the cell-edge region is only capable of receiving the base layer due to its lower receive SNR. The design goal of [42] was to sacrifice the performance of the cell-edge region for the sake of improving the power-efficiency of the broadcast system, where both the base and enhancement layers may be broadcast simultaneously, but the reception of the two types of information may be separated.

In 2001, Vitthaladevuni [43] analysed the BER computation of the M-QAM HM constellations. He commenced this discourse by describing the generation rule of several specific HM constellations exhibiting different protection levels. Then, the BER performance of his uncoded HM based QAM constellation was characterized mathematically for transmission over AWGN channels based on the Gaussian Q-function, including HM-16QAM, HM-64QAM, as well as HM-256QAM. The general BER expressions of 4/M-QAM constellations have also been discussed in the context of AWGN channels. Furthermore, the derivation of the BER performance of the family of 4/M-QAM constellations was extended to flat-fading channels.

A whole suite of various channel coding as well as source coding schemes were conceived in [15], [21], [52], [53], [55], and [57]. The design problems as well as the associated challenges of HM based schemes are illustrated in Fig. 4. During 2013 to 2015, the authors of this treatise have also investigated the performance of coded HM based cooperative

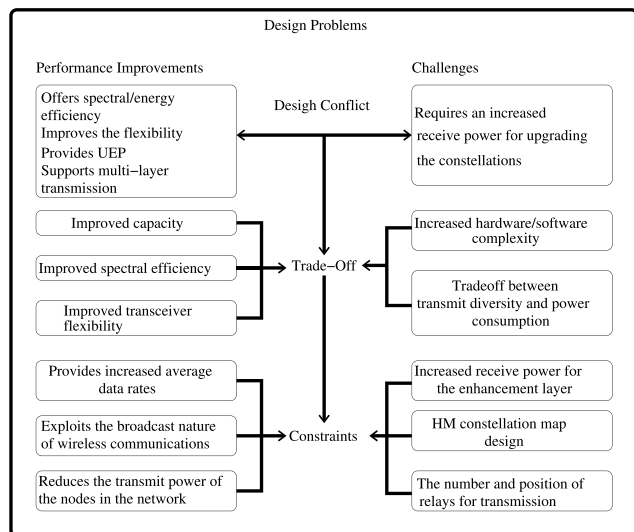


FIGURE 4. Challenges in the design of HM based schemes.

communications [58]–[61] with the objective of reducing both the complexity as well as the power consumption of the entire cooperative communication system. To be more specific, in [60], we employed a system architecture similar to that of Hausl and Hagenauer [17]. Additionally, the specific constellation map of the HM scheme was also taken into consideration, when minimizing the power consumption of the entire system. However, in order to improve the flexibility of the system conceived in [60], we invoked HM for supporting the transmission of multiple independent channel coded signals in [58], [59], and [61], where both the constellation map of the HM as well as the position of the RN were jointly considered. Furthermore, in [59], we characterized the lower performance bound of our HM aided cooperative scheme based on the Discrete-Input Continuous-Output Memoryless Channel (DCMC) capacity and under the assumption that a ‘perfect channel capacity achieving’ code is employed. Based on the results in [58]–[61], we concluded that by employing an appropriate cooperative HM scheme, both the flexibility as well as the power-efficiency of the entire cooperative system can be improved. We also demonstrated that the system structure proposed in [58]–[61] may be readily employed in wireless *ad hoc* networks. This observation inspired us to intrinsically amalgamate the coded HM scheme with Opportunistic Routing (OR) in the context of *ad hoc* networks for the sake of reducing the power consumption of the entire networks as it will be crystallized in our novelty statement at the end of the next section.

III. OPPORTUNISTIC ROUTING IN AD HOC NETWORKS

In their embryonic era, wireless *ad hoc* networks were referred to as ‘packet radio’ networks, which were primarily designed by the Advanced Research Project Agency (DARPA) during the 1970s. The history of wireless *ad hoc* networks is eloquently portrayed for example in

Labiod’s book [62]. The most significant benefit of *ad hoc* networks is their distinctively flexible nature. An *ad hoc* network relies on multiple nodes, which are connected by ‘links’. The communication between any two nodes in the *ad hoc* network may be assisted by all the other nodes in the network relying on a specific transmit power, path-loss, fading and noise characteristics. A series of links which connect a set of communication nodes is termed as a ‘path’. Since the links among the nodes in the network may become disconnected at any time, a resilient network must be capable of dynamically restructuring itself with the aid of reliable routing methods invoked for finding beneficial paths [63] for the transmissions. Therefore, the research of *ad hoc* networks has been mainly focussed on the conception of diverse routing algorithms. Table 2 summaries the milestones in the research of wireless *ad hoc* networks during the past twenty years.

A detailed investigation of position-based routing in mobile *ad hoc* networks was disseminated in 2001 by Mauve [83]. More explicitly, the associated transmission protocols [65], [67]–[69], [72], [75]–[78], the routing algorithms [64], [66], [71], [74], [79] as well as the capacity [70], [73], [80] and energy efficiency [80], [81] were lavishly characterized in the open literature. More recently, the family of OR algorithms has inspired increasing research attention [84]–[88]. The route selection algorithm of the network layer of wireless communications is simply referred to as the routing algorithm. Traditional Routing (TR) algorithms, such as dynamic source routing and *ad hoc* on-demand distance vector routing [71], [89]–[91], may select one or more optimized fixed routes before transmissions. Once, the transmissions commence, the selected route must not be changed until the next transmission Time Slot (TS). The TR algorithm may select a specific route based on the quality of the current channel states or motivated by the low geographic distance among the candidate RNs. However, the TR algorithm may not be capable of adapting sufficiently promptly to dynamic wireless environments due to the rapid fluctuation of the channel conditions [92] in high-velocity scenarios, such as Vehicular *Ad Hoc* Networks (VANETs), for example. Nonetheless, the TR algorithm may result in a preponderance of retransmission attempts in wireless communications, which may lead to a waste of network resources or even to dropped sessions [81]. With the exponential growth of the number of wireless communication devices, new routing algorithms are required for supporting heterogeneous networks and wireless devices in order to overcome the limitations of the TR algorithms. Hence, Opportunistic Routing (OR) algorithms have been developed [71], [84]–[88], [93], [94], which typically rely on the following four steps:

- 1) Candidate relay selection;
- 2) Packet broadcast to the candidate relays;
- 3) Relay selection for packet forwarding;
- 4) Packet forwarding.

In contrast to TR algorithms, the family of OR algorithms typically exploits the broadcast nature of wireless

TABLE 2. Milestones in wireless *ad hoc* networks (1994-2015).

Year	Author(s)	Contribution
1994	Johnson [66]	Route discovery and route maintenance protocol for <i>ad hoc</i> networks
1995	Davies <i>et al.</i> [67]	Contention-tree based multiple access method for <i>ad hoc</i> wireless networks
1997	Das and Bharghavan [68]	Employ virtual backbone structure into <i>ad hoc</i> networks for route searching
1999	Broch <i>et al.</i> [69]	Integrated <i>ad hoc</i> nodes into the hierarchical Internet for mobile transmission
2000	Jonsson <i>et al.</i> [70]	Connect an <i>ad hoc</i> network to the Internet by using mobile IP
2001	Niculescu and Nath [71]	Estimated the approximate location of all nodes in <i>ad hoc</i> networks
2002	Gorssglauser and Tse [72]	Investigated the capacity and throughput of an <i>ad hoc</i> network
2003	Zorzi and Rao [73]	Conceived a forwarding algorithm for <i>ad hoc</i> and sensor network
2004	Younis and Fahmy [74]	Conceived a protocol for supporting scalable data aggregation in <i>ad hoc</i> sensor networks
2005	Weber <i>et al.</i> [75]	Estimate the capacity of wireless <i>ad hoc</i> network with outage constraints
2006	Pelusi <i>et al.</i> [76]	Conceived opportunistic data forwarding for <i>ad hoc</i> networks
2008	Zhao and Cao [77]	Vehicle-assisted data delivery in <i>ad hoc</i> networks
2009	Harri <i>et al.</i> [78]	Mobility models were proposed for vehicular <i>ad hoc</i> networks
2010	Tonguz <i>et al.</i> [79]	A distributed vehicular broadcast protocol was conceived for <i>ad hoc</i> networks
2011	Kim and Giannakis [80]	Resource allocation was designed for MIMO <i>ad hoc</i> cognitive radio Networks
2012	Bhorkar <i>et al.</i> [81]	Adaptive OR was designed for wireless <i>ad hoc</i> networks
2013	Huang [82]	The throughput of mobile <i>ad hoc</i> networks relying on energy harvesting was studied
2014	Zuo <i>et al.</i> [83]	Energy-efficient cross-layer OR algorithms were designed for <i>ad hoc</i> networks
2015	Sharma and Kumar [84]	Opportunistic cross layer design for airborne <i>ad hoc</i> networks

communications, where the receiver may be chosen from the full set of nodes in the network, which are capable of flawlessly receiving the packets. Note that among all the candidate relay nodes, the one which is geographically closest to the DN is most likely to be chosen for forwarding the packet during the next transmission [93]. Since multiple candidates are available for receiving the broadcast packet, the probability of at least one candidate correctly receiving the packets may be improved. Hence, the reliability, the throughput, as well as the power efficiency of the entire system may be improved with the aid of OR algorithms. The evolution and history of OR algorithms is summarized in Table 3.

In order to overcome the deficiencies of conventional routing [71], [89]–[91], meritorious Opportunistic Routing (OR) algorithms have been developed in [71], [79], [81], [85]–[89], [93], [94], [114], and [127]–[131], which exploit the broadcast nature of wireless transmissions and the beneficial path diversity of the multi-hop wireless networks [85]. In contrast to conventional routing, OR relies on multiple opportunistic paths for forwarding the packets [88]. The receiver of the next hop in OR is dynamically chosen from all the nodes in the network, which are likely to correctly receive the packet. This receiver node is typically the one, which is geographically closest to the Destination Node (DN) [93]. Since multiple forwarding candidates are activated for assisting the packet's passage through the network, the probability of at least one candidate correctly receiving the packet is increased compared to conventional routing [85]. Given the increased reliability of each hop's transmission, both the throughput and the energy-efficiency of the entire system may be improved [81], [85], [114]. The so-called Extremely Opportunistic Routing (ExOR) regime of [86] is one of

the primary OR algorithms in the literature [88]. Explicitly, the ExOR algorithm carries the forwarder node-index list information in the header of the broadcast packets and the specific nodes, which have successfully received the packet are likely to be used as the transmitter during the following Time Slot (TS). Apart from the ExOR algorithm, numerous other opportunistic strategies have been developed for solving diverse problems, such as Geographic Random Forwarding (GeRaF) algorithm of [71] and [94] and the MAC-agnostic opportunistic routing of [87]. However, the key objective of all OR strategies is more or less the same, namely that of finding the best candidates in the cooperative network for forwarding the signal. At the time of writing, researchers tend to focus their attention on the specific characteristics of OR algorithms, such as their energy consumption [81], [114], [130], [132], their system delay [81], [131] and system capacity/throughput bound [85]. However, despite having numerous research papers on OR, there is a paucity of analytical studies on the performance of cooperative networks relying on OR algorithms [93], especially in the context of HM.

Against this backdrop, our contribution is the conception of a new cooperative communication paradigm relying on TTCM-aided twin-layer HM-16QAM. The layered modulated packets are forwarded through the cooperative network using our OR algorithm. However, instead of conveying the layered modulated packets as an inseparable unit, our OR scheme beneficially exploits the specific features of the HM scheme. More specifically, the twin-layer HM-16QAM signal packets are partitioned into a pair of sub-packets, which may become separately broadcast, depending the near-instantaneous received power of all the potential receiver

TABLE 3. Milestones in opportunistic routing (2003-2015).

Year	Author(s)	Contribution
2003	Zorzi and Rao [73]	Geographic random forwarding (GeRaF) algorithm
	Fussler <i>et al.</i> [97]	Contention-based forwarding for mobile networks
2004	Zhao <i>et al.</i> [98]	GeRaF aided hybrid-ARQ for <i>ad hoc</i> networks
	Biswas and Morris [99]	OR algorithm in multi-hop wireless networks
2005	Yuan <i>et al.</i> [100]	Resilient opportunistic mesh routing algorithm
	LeBrun <i>et al.</i> [101]	Knowledge-based OR in wireless <i>ad hoc</i> networks
	Biswas and Morris [88]	Extremely Opportunistic Routing (ExOR) algorithm
2006	Westphal [102]	OR algorithm in dynamic <i>ad hoc</i> networks
	Rozner <i>et al.</i> [103]	Simple OR protocol for wireless mesh networks
	Zhong <i>et al.</i> [104]	Candidates selection for opportunistic path forwarding
2007	Zeng <i>et al.</i> [105]	Throughput of geographic OR algorithm
	Nassr <i>et al.</i> [106]	Scalable and reliable sensor network routing
	Chachulski <i>et al.</i> [89]	Trading structure for random OR algorithm
2008	Lin <i>et al.</i> [107]	OR with segmented network coding (CodeOR)
	Koutsonikolas <i>et al.</i> [108]	Synergistic interflow network coding and OR
	Conan <i>et al.</i> [109]	Fixed point OR in delay tolerant networks
2009	Zeng <i>et al.</i> [110]	Location-aided OR in multirate and multihop networks
	Yang <i>et al.</i> [111]	Position based OR algorithm
	Laufer <i>et al.</i> [112]	Multirate routing in wireless mesh networks
2010	Lin <i>et al.</i> [113]	Online opportunistic network coding aided by SlideOR
	Naghshvar and Javidi [114]	OR with congestion diversity in multi-hop networks
	Bletsas <i>et al.</i> [115]	Interference limited OR in reactive sensing
2011	Mao <i>et al.</i> [116]	Energy-efficient OR in wireless sensor networks
	Lee and Hwang [117]	Minimum energy cost design of a two-hop networks
	Lee and Haas [95]	OR for short-haul multi-hop networks
	Fang <i>et al.</i> [118]	Node-constrained OR in wireless mesh networks
2012	Bhorkar <i>et al.</i> [81]	Adaptive OR for wireless <i>ad hoc</i> networks
	Lampin <i>et al.</i> [119]	QoS oriented OR protocol for sensor networks
	Wang <i>et al.</i> [120]	Cooperative OR in mobile <i>ad hoc</i> networks
2013	Guo <i>et al.</i> [121]	Opportunistic flooding with unreliable links
	Xiao <i>et al.</i> [122]	Time-sensitive OR in delay tolerant networks
	Shin <i>et al.</i> [123]	Parallel OR in wireless networks
2014	Zuo <i>et al.</i> [83]	Cross-layer energy-efficient OR algorithm
	Zhong <i>et al.</i> [124]	Coding-aware OR in cognitive radio networks
	Xiao <i>et al.</i> [125]	Community-aware OR in mobile social networks
2015	Chen <i>et al.</i> [126]	Theoretical analysis of buffer-aided OR
	Wu <i>et al.</i> [127]	Game-theoretic based OR in wireless networks
	Elias <i>et al.</i> [128]	Contest-aware OR for stationary sensor networks

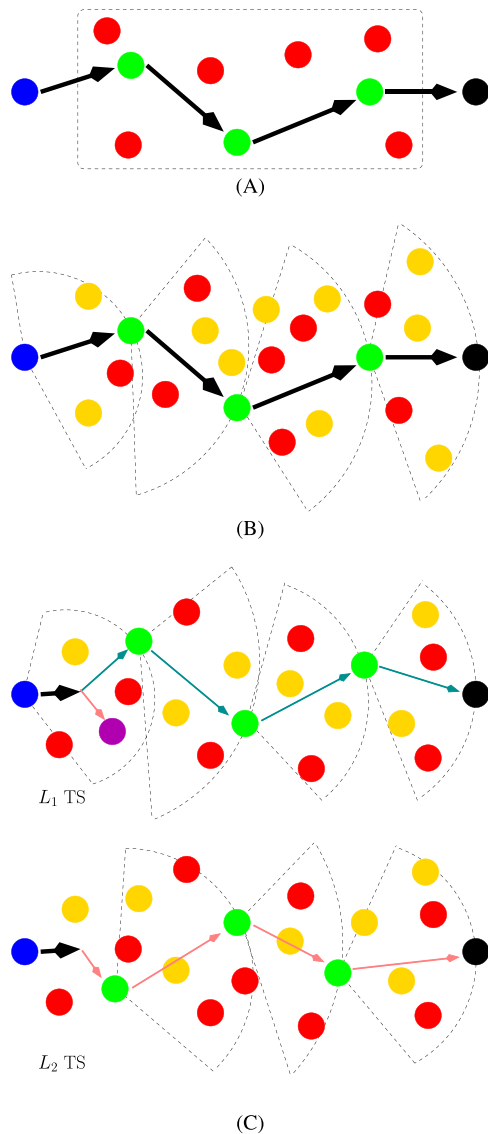
node candidates. The OR-aided benchmark algorithm, which always keeps the layered modulated packets together as an inseparable integral unit during its transmission will be referred to as the Traditional OR (TOR) algorithm. By contrast, our HM aided OR algorithm is termed as Hierarchical Modulated Opportunistic Routing (HMOR).

IV. SYSTEM MODEL

The comparisons among the TR, TOR and HMOR are illustrated in Fig. 5. The route for the TR algorithms is decided before the commencement of transmissions. By contrast, for the TOR algorithms, multiple receive candidates will be chosen before each broadcast phase and then the specific RN transmitter activated for forwarding the information during the following TS will be selected according to specific decision algorithms. Even though the transmitted packet is formed by twin-layer HM-16QAM symbols, both the TR and the TOR algorithms will always deliver the layered modulated packets as an inseparable integral payload unit. In contrast to this inseparable delivery philosophy, our HMOR algorithm may partition the packets into a pair of sub-packets, namely L_1 and L_2 . The route selection algorithm

of our HMOR algorithm is the same as that of the TOR algorithms, but when the packet becomes partitioned into L_1 and L_2 , the entire network may be configured to focus on forwarding the high-priority base-layer L_1 first. When L_1 is received by the DN, the network will start the transmission of L_2 . By partitioning the twin-layer HM-16QAM based packet into a pair of sub-packets, the packets that are forwarded through the network will require a lower receive power due to the reduced constellation size. Hence the transmit power of each node in the network may be reduced.

In order to simplify the discussions, our analysis provided in this treatise is mainly focussed on a cooperative system assisted by two RNs. The general system model is illustrated in Fig. 6. Although the entire system only has two hops, our transmission algorithm can be readily extended to a larger network. Explicitly, this simple network already characterizes most of the typical situations of a large network having more than three hops. Note that the first RN (RN_1) is near to the SN and the second RN (RN_2) is near to the DN. During the first TS, the SN will broadcast a signal frame to all the other nodes of the cooperative network, where both RN_1 and RN_2 are willing to forward the information to the DN.



- SN: ● DN: ●
- RN: ● Transmission failed
- Transmission succeeded, but the node is not chosen to be the forwarder
- Transmission succeeded and the node is chosen to be the forwarder
- The node is waiting for forwarding L_2
- Twin-Layer HM info.: \blackrightarrow (4 bits/symbol)
- L_1 info.: \rightarrow (2 bits/symbol)
- L_2 info.: \rightarrow (2 bits/symbol)

FIGURE 5. Comparison of TR, TOR and HMOR. (A) Traditional routing. (B) Traditional opportunistic routing (TOR). (C) Twin-layer HM aided OR (HMOR).

Additionally, the pair of RNs also collaborate with each other during the transmissions. The original signal frame received from the SN contains a pair of independent layers,

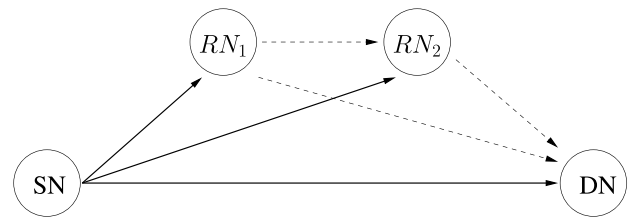


FIGURE 6. The model of our twin-relay assisted cooperative system.

which are originally conveyed together by the HM scheme. We denote the layer with a higher protection priority as L_1 , while that having a lower protection level as L_2 . According to the specific features of the HM scheme, the SNR required by receiver for decoding L_1 is lower than that of L_2 . Hence, upon receiving the twin-layer HM signals, we assume that if the node in the cooperative network is capable of successfully receiving L_2 , it is also capable of receiving L_1 at an adequate integrity.

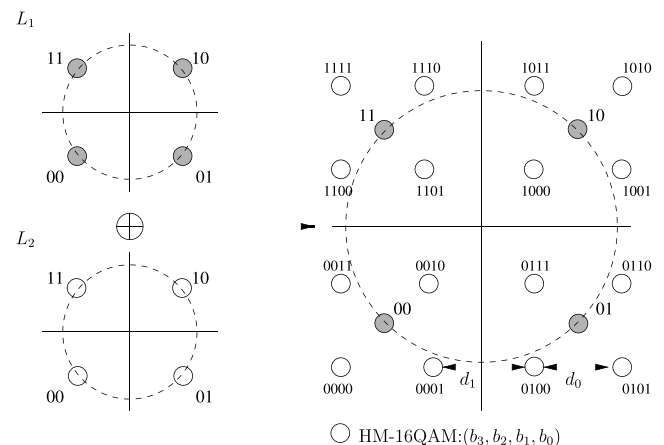


FIGURE 7. The constellation map of the HM scheme, where $R_1 = d_1/d_0$.

The constellation map of our HM-16QAM scheme is shown in Fig. 7, which was repeated from [59] for convenience. Further details of our twin-layer HM scheme are also available in [59]. We define the four bits of a HM-16QAM symbol as $(b_3b_2b_1b_0)$, where L_1 is defined by (b_3b_2) , while (b_1b_0) are contained in L_2 . Both of the two layers are encoded by a rate-1/2 TTCM encoder. Hence, there is one information bit and one parity bit in each layer. The generation rule of the twin-layer HM-16QAM symbols may be formulated as:

$$S_{HM-16QAM} = \frac{1 + R_1}{\sqrt{1 + (1 + R_1)^2}} \left[S_{4QAM} \pm \frac{1}{(1 + R_1)} e^{\pm \frac{\pi}{4} j} \right], \quad (1)$$

where S_{4QAM} denotes the conventional square 4QAM constellations and the HM-16QAM ratio $R_1 = d_1/d_0$ is defined in [59] for controlling the shape of the HM-16QAM constellations, which has the constraint of $R > 0$, as detailed in [59]. We have found in [59] that the optimum performance of the system is achieved, when the HM-16QAM ratio is

$R_1 = 3.0$, while the rate-1/2 TTCM decoder has $\zeta = 4$ decoding iterations and the transmission packet size is $\eta = 12,000$ symbols. It is worth mentioning that we opted for a high interleaver length of $\eta = 12,000$ in [59] for the sake of achieving a high performance in the physical layer. However, a transmission packet length of $\eta = 12,000$ symbols may be excessive under the assumption that the fading channels' envelope remains constant during each packet's transmission in a specific link. Hence, in this study, the settings of the HM ratio R_1 and the rate-1/2 TTCM encoder/decoder were the same as those in [59], but the packet length was reduced to $\eta = 1,200$ symbols.

TABLE 4. Simulation parameters used in the TTCM-aided twin-layer HM base HMOR schematic of Fig. 6.

Coded Modulation	TTCM
Modulation Scheme	4QAM, HM-16QAM
HM ratio R_1	3.0
Mapper type	Set-Partitioned
Number of iterations	4
Code Rate	1/2
Code Memory	3
Code Polynomial (octal)	$H_{4QAM} = [13\ 06]$
Decoder type	Approximate Log-MAP
Symbols per frame	1,200
Number of frames	10,000
Channel	AWGN channel Rayleigh-distributed block fading channel
Path-loss exponent	2

V. THEORETICAL ANALYSIS

The structure of this long section may be seen at a glance in Fig. 3. Again, the system considered communicates over Rayleigh-distributed block fading channels, where all nodes of the cooperative network are assumed to benefit from perfect Channel State Information (CSI). The related simulation parameters are shown in Table 4. Furthermore, the symbols used in this section are defined as follows:

- \mathbb{P}_t : the transmit power.
- \tilde{h} : the instantaneous channel fading value.
- $\bar{\gamma}$: the average receive SNR, which is $\bar{\gamma} = \frac{\mathbb{P}_t \kappa}{N_0 d^\alpha}$, where $\kappa = \left(\frac{c}{4\pi f_c}\right)^2$ is a constant, while c is the speed of light, $f_c = 2.4\text{ GHz}$ is the carrier frequency according to the WIFI standards, d denotes the distance and α is the path-loss exponent. Specifically, we consider the classic free-space path-loss model [133], [134], where we have $\alpha = 2$ and N_0 is the noise power, which is set to -110 dBm in our simulations.
- γ : the instantaneous receive SNR, which is given by $\gamma = \tilde{h}\bar{\gamma}$.
- N_t the number of maximum transmission attempts for each node in the cooperative network.

A. FER DERIVATION

Evaluating the FER metric is vital for determining whether the information is received successfully or not, which depends on many numerous factors, including the AWGN,

the channel fading, the path-loss, etc. Although we can directly infer the FER performance of a specific channel coding scheme in a given scenario with the aid of Monte-Carlo simulations, in order to investigate our OR-assisted cooperative scenario, we have to characterize the FER as a function of the receive SNR γ . A similar technique has been conceived for a single-layer transmission scenario in [81]. In this treatise, we employ the TTCM aided twin-layer HM scheme of Fig. 7. We firstly generate the FER versus SNR curve for transmission over AWGN channels using simulations and then invoke the schemes designed in [135] to find accurately matching polynomials for characterizing the FER versus SNR curve. As seen in Table 4, the coding rate of the TTCM scheme used in this treatise is set to $R_C = 0.5$, with a block length of $\eta = 1,200$ symbols, while the octally represented generator polynomials of the rate-1/2 TTCM encoder are [13 06]. According to the simulation-based FER versus SNR curve of the AWGN channel, the following three-segment FER versus SNR model is constructed for representing the performance of the twin-layer TTCM aided transmission over AWGN channels:

$$FER_{AWGN}(\bar{\gamma}) \approx \begin{cases} 1 & \text{if } 0 \leq \bar{\gamma} < \eta_1, \\ \sum_{k=1}^4 a_k(\bar{\gamma})^{4-k} & \text{if } \eta_1 \leq \bar{\gamma} < \eta_2, \\ a_5 e^{-10a_6 \log_{10}(\frac{\bar{\gamma}}{\Delta})} & \text{if } \bar{\gamma} \geq \eta_2. \end{cases} \quad (2)$$

In AWGN channels we have $\tilde{h} = 1$, hence, $\gamma = \bar{\gamma}$. Explicitly, we divide the FER_{AWGN} versus SNR simulation curve of Eq. (2) into three segments according to the received SNR thresholds η_1 and η_2 . During the fitting process carried out by Matlab, the appropriate values of η_1 and η_2 may be obtained. Additionally, Δ is a variable we used for simplifying the Matlab-based curve-fitting process. Then the FER versus SNR performance encountered over Rayleigh-distributed block fading channels may now be expressed as:

$$FER_{Rayleigh}(\tilde{h}\bar{\gamma}) = \int_0^\infty e^{-\tilde{h}} FER_{AWGN}(\tilde{h}\bar{\gamma}) d\tilde{h}. \quad (3)$$

Hence, we have the following scenario:

- When $0 \leq \tilde{h}\bar{\gamma} < \eta_1$, we arrive at:

$$FER_{Rayleigh}^I = \int_0^{\frac{\eta_1}{\bar{\gamma}}} e^{-\tilde{h}} d\tilde{h} = 1 - e^{-\frac{\eta_1}{\bar{\gamma}}}. \quad (4)$$

- For $\eta_1 \leq \tilde{h}\bar{\gamma} < \eta_2$, we have:

$$\begin{aligned} FER_{Rayleigh}^{II} &= \int_{\frac{\eta_1}{\bar{\gamma}}}^{\frac{\eta_2}{\bar{\gamma}}} \sum_{k=1}^4 a_k(\tilde{h}\bar{\gamma})^{4-k} e^{-\tilde{h}} d\tilde{h} \\ &= \sum_{k=1}^4 a_k \bar{\gamma}^{4-k} \int_{\frac{\eta_1}{\bar{\gamma}}}^{\frac{\eta_2}{\bar{\gamma}}} \tilde{h}^{4-k} e^{-\tilde{h}} d\tilde{h} \\ &= \sum_{k=1}^4 a_k \bar{\gamma}^{4-k} \left[\gamma(5-k, \frac{\eta_2}{\bar{\gamma}}) - \gamma(5-k, \frac{\eta_1}{\bar{\gamma}}) \right], \end{aligned} \quad (5)$$

TABLE 5. Curve-fitting parameters for the FER versus SNR performance of receiving rate-1/2 TTCM 4QAM scheme, and of receiving L_1 and L_2 of the TTCM aided twin-layer HM-16QAM scheme given HM ratio of $R = 3.0$. The related parameters for the channel coding schemes employed are shown in Table 4.

	Parameters
Transmitting Rate-1/2 4QAM TTCM	$\eta_1 = 1.1480e + 00, \eta_2 = 1.4125e + 00, \Delta = 1$ $a_1 = 9.6418e + 01, a_2 = 3.7845e + 02, a_3 = 4.9016e + 02$ $a_4 = -2.0888e + 02, a_5 = 7.8800e + 03, a_6 = 7.3000e + 00$
Transmitting L_1 Twin-layer HM-16QAM TTCM aided	$\eta_1 = 1.1480e + 00, \eta_2 = 1.6218e + 00, \Delta = 1$ $a_1 = 3.9603e + 01, a_2 = -1.7931e + 02, a_3 = 2.6689e + 02$ $a_4 = -1.2998e + 02, a_5 = 9.2100e + 03, a_6 = 5.2000e + 00$
Transmitting L_2 Twin-layer HM-16QAM TTCM aided	$\eta_1 = 1.9500e + 01, \eta_2 = 2.4547e + 01, \Delta = 15$ $a_1 = 1.5429e - 02, a_2 = -1.0273e + 00, a_3 = 2.2521e + 01$ $a_4 = -1.6192e + 02, a_5 = 8.0000e + 05, a_6 = 7.6000e + 00$

where $\gamma(s, x) = \int_0^x t^{s-1} e^{-t} dt$, which is the lower incomplete gamma function.

- Finally, for $\tilde{h}\bar{\gamma} \geq \eta_2$, we arrive at:

$$\begin{aligned}
 FER_{Rayleigh}^{III} &= \int_{\frac{\eta_2}{\bar{\gamma}}}^{\infty} a_5 e^{(-10a_6 \log_{10}(\frac{\tilde{h}\bar{\gamma}}{\Delta}))} e^{-\tilde{h}} d\tilde{h} \\
 &= a_5 e^{-10a_6 \log_{10}(\frac{\bar{\gamma}}{\Delta})} \left(\frac{\eta_2}{\bar{\gamma}}\right)^{\left(1 - \frac{10a_6}{\ln 10}\right)} \\
 &\quad \times G_{1,2}^{2,0} \left[\frac{\eta_2}{\bar{\gamma}} \middle| \frac{10b}{\ln 10} - 1, 0 \right], \quad (6)
 \end{aligned}$$

where, we have $G_{1,2}^{2,0} \left[x \middle| \frac{\nu}{\nu - 1}, 0 \right] = E_{\nu}(x) = \int_1^{\infty} \frac{e^{-xt}}{t^{\nu}} dt$, which is the Meijer-G function defined in [136] and [137].

Therefore, the FER versus SNR performance for transmission over Rayleigh-distributed block fading channels is given by:

$$\begin{aligned}
 FER_{Rayleigh}(\gamma\bar{\gamma}) &= FER_{Rayleigh}^I + FER_{Rayleigh}^{II} \\
 &\quad + FER_{Rayleigh}^{III}. \quad (7)
 \end{aligned}$$

Quantitatively, in our simulations of Fig. 8, there are six FER versus SNR curves that have to be matched. We have two curves for the FER versus SNR performance of the rate-1/2 TTCM coded 4QAM scheme for transmission over both AWGN channel and Rayleigh-distributed block fading channels, another two curves for receiving L_1 of the twin-layer rate-1/2 TTCM aided HM scheme over the two channels, and the last two curves for receiving L_2 of the twin-layer rate-1/2 TTCM aided HM scheme over the two channels. The related curve-fitting parameters are shown in Table 5.

It can be observed from Fig. 8(a) and Fig. 8(b) that our mathematical FER versus SNR curve fitting schemes indeed match the simulation curves of the FER versus SNR performance over both AWGN and Rayleigh-distributed block fading channel. Therefore, we have successfully characterized the FER performance as a function of the instantaneous receiver SNR. By computing the FER versus SNR performance curves for both the AWGN and Rayleigh-distributed block fading channel, we arrive at the nodes' successful reception probability based on their near-instantaneous receiver SNR. Therefore, both their power-efficiency and delay may now be quantified. In the following section, we

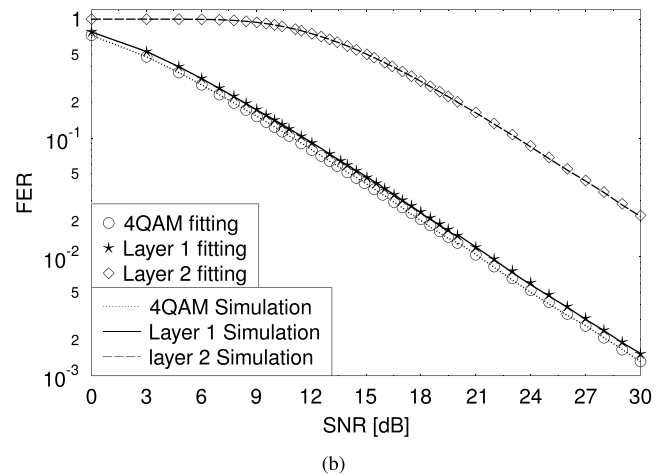
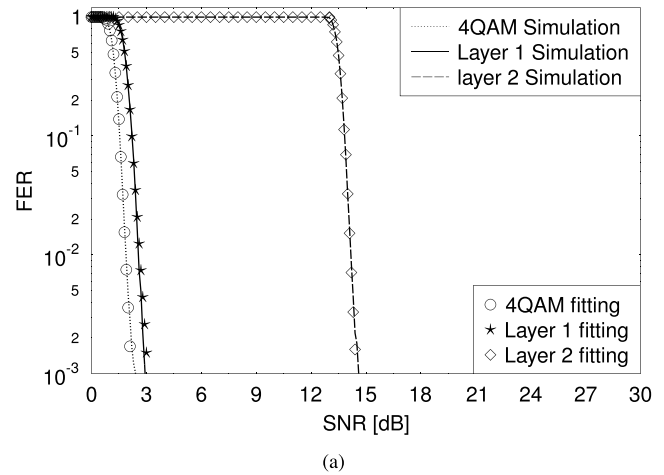


FIGURE 8. The BER versus FER performance of receiving rate-1/2 TTCM 4QAM scheme, and of receiving L_1 and L_2 of the TTCM aided twin-layer HM-16QAM scheme given HM ratio of $R = 3.0$. The curve-fitting parameters are shown in Table 5 and the related simulation parameters are shown in Table 4. (a) AWGN channel. (b) Rayleigh-distributed block fading channel.

have listed the ten possible states in our cooperative transmissions regime and the basic transmission activation rules among the nodes for the theoretical performance analysis of our system.

B. LEGITIMATE SYSTEM STATES AND STATE TRANSITIONS

Let us now characterize our four-node cooperative communication network in terms of its ten states of $\{S_i\}$, where we have

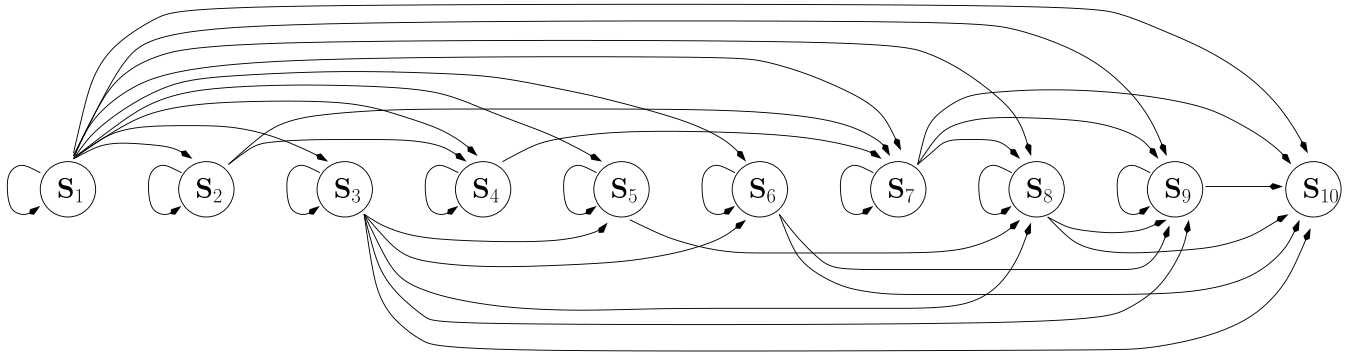


FIGURE 9. The state transition diagram of the ten legitimate system states of the cooperative schematic of Fig. 6.

$i \in \{1, 2, \dots, 10\}$. The ten states are shown in Table 6, whilst their state-transitions will be discussed below with reference to Fig. 9.

TABLE 6. The ten states of the TCM aided twin-layer HM-16QAM based twin-relay assisted cooperative communication system of Fig. 6. Explicitly, the L_1 and L_2 indicate the information received by each of the four nodes in specific state.

State	SN	RN ₁	RN ₂	DN
S ₁	L_1, L_2			
S ₂	L_2	L_1		
S ₃		L_1, L_2		
S ₄	L_2		L_1	
S ₅		L_2	L_1	
S ₆			L_1, L_2	
S ₇	L_2			L_1/Null
S ₈		L_2		L_1/Null
S ₉			L_2	L_1/Null
S ₁₀				$L_1/\text{Null}, L_2/\text{Null}$

As shown in Table 6, each state illustrates the current buffer status of each node in the network. We define the node nearest to the DN that receives L_1 or L_2 , as the ‘Frontier’ of L_1 or L_2 , where only the node which is the ‘Frontier’ of L_1 or L_2 or both may be chosen to be the transmitter for forwarding the packet during the following transmission. Since after every transmission the ‘Frontier’ of L_1 or L_2 are unique, we use the ‘Frontier’ of L_1 and L_2 to define the specific receiver state of the system and produce Table 6. Due to the specific layer-based decoding feature of the HM scheme, L_1 having a higher protection level requires a lower receiver SNR than that of L_2 . Therefore, the position of the particular RN, which successfully received L_2 will never be beyond the position of that RN, which successfully received L_1 . Hence, if there are n nodes in the network, the total number N_{state} of the legitimate system states may be expressed as:

$$N_{state} = 1 + 2 + \dots + n = \frac{n(n+1)}{2}. \quad (8)$$

Note that during any transmission, only one of the nodes in the network is activated for transmission, which corresponds to a Time Division Multi Access (TDMA)-style multiple access. For a specific node, if a packet encounters

a transmission outage N_t times, then the packet will be discarded. To be more specific, the transition among the legitimate system states are presented in Fig. 9, and the details of the ten states of the four-node network are described below with the aid of frequent references to Fig. 9:

- **State S₁**: it is the initial ‘switch-on’ state or the state, when all the other nodes in the cooperative network failed to receive even a single layer information from the SN. Hence, the SN may have to retransmit both the L_1 and L_2 layers during the following TS. Note that if the current state is S₁, the next state may be any one of all the then legitimate states. We have to mention that if the current state is the same as the following state, this implies that the transmission attempt of the current state has failed, hence the packet has to be retransmitted, as seen in Fig. 9.
- **State S₂**: only RN₁ is capable of receiving L_1 . Here, we allow RN₁ to have the necessary priority to transmit its L_1 first, during the forthcoming TS. Only when the DN has received L_1 or if L_1 is discarded, because if the number of transmission attempts exceeds N_t , then SN will be allowed to retransmit L_2 . Therefore, the next state arrived at from S₂ may be S₂, S₄ or S₇, as portrayed in Fig. 9.
- **State S₃**: both L_1 and L_2 are received by the RN₁. Hence, during the following TS, SN could remain silent, while RN₁ may attempt to forward L_1 and L_2 to the DN. Therefore, the observe also in Fig. 9 that next state transition from S₃ may be S₃, S₅, S₆, S₈, S₉ or S₁₀.
- **State S₄**: RN₂ is capable of receiving L_1 , while both RN₁ and RN₂ failed to receive L_2 and DN also receives nothing. In this situation, since RN₂, which is nearer to the DN successfully decoded L_1 , during the next TS, the system will only allow RN₂ to forward L_1 to DN. After RN₂ completed its transmission, SN will commence its retransmission of L_2 . Hence the state S₄ may be followed by S₄ or S₇, as visualized in Fig. 9.
- **State S₅**: RN₂ is capable of receiving L_1 , while RN₁ successfully decodes both L_1 and L_2 , but DN fails to receive anything. Then RN₂ will attempt to transmit L_1 to DN in the following TS, and after it completed its

transmission, RN₁ will be activated in order to forward L₂ without L₁. The following state upon emerging from S₅ of Fig. 9 will be S₅ or S₈.

- **State S₆**: RN₂ is capable of receiving both layers L₁ and L₂, while DN received nothing. In this situation, RN₂ will forward both of L₁ and L₂ to DN during the following TS, while the SN and RN₁ will remain silent until the system starts to transmit its next package. As seen in Fig. 9, the following state upon emerging from S₆ will be S₆, S₉ or S₁₀.
- **State S₇**: this state may be reached from S₁, S₂, S₄ and S₇, depending on two situations, namely on whether DN has received L₁ and on whether the system has discarded L₁ due to N_t failed transmission attempts. Let us consider the transition S₄ → S₇ for instance. If the previous state is S₄, then RN₂ may forward L₁ to DN, provided that DN successfully receives L₁. Then the system will traverse to state S₇, since DN received L₁ and the entire system will only attempt to forward L₂ to DN from SN during the following TS. However, if RN₂ failed to successfully transmit L₁ to DN, the following state will still be S₄. Then RN₂ will try to retransmit L₁, but if reception failures occur for N_t times, then RN₂ has to discard L₁ and allow SN to retransmit L₂. Hence, a state transition of Fig. 9 will be enforced from S₄ to S₇ with DN marked by the flag L₁ lost, as the ‘Null’ in Table 6. The state transitions emerging from S₇ may be S₇, S₈, S₉ or S₁₀.
- **State S₈**: similar to S₇, DN may either have successfully received L₁ or L₁ may have been discarded, which depends on the previous state. Meanwhile, L₂ will be forwarded to DN by RN₁ during the following TS. The following states reached from S₈ may be S₈, S₉ or S₁₀.
- **State S₉**: similar to S₇, in the following TS, only RN₂ is activated to forward L₂ to DN. The next state upon departure from S₉ be S₉ or S₁₀, as observed in Fig. 9.
- **State S₁₀**: the final state for each packet’s transmission, while, whether that layer L₁ or L₂ may be successfully received by the DN or be discarded still depends on the previous state.

C. SINGLE-STEP STATE-TRANSITION PROBABILITY

During the transmissions, SN and RN may have to transmit two types of signals. More specifically, when they have to forward all of the twin-layer information, they would transmit the HM-16QAM symbols streams. By contrast, when they only have to forward single-layer information (L₁ or L₂), they would transmit rate-1/2 4QAM TCM coded symbols. Hence, according to the analysis in Section V-A, we define the following state-transition probabilities:

- P^{4QAM} : The probability of successfully receiving the rate-1/2 TCM 4QAM symbols, which is given by $P^{4QAM} = 1 - FER^{4QAM}(\gamma)$.
- P^{L_1} : The probability of successfully receiving L₁, when the HM-16QAM signals were transmitted, which is formulated as $P^{L_1} = 1 - FER^{L_1}(\gamma)$.

- P^{L_1, L_2} : The probability of successfully receiving both L₁ and L₂, when the HM-16QAM signal was transmitted (as mentioned before, when the node is capable of receiving L₂, it may also be able to successfully receive L₁). It is expressed as $P^{L_1, L_2} = 1 - FER^{L_1, L_2}(\gamma)$.
- $P^{[0/2]}$: The probability of transmitting the twin-layer HM-16QAM signals, but both L₁ and L₂ were received unsuccessfully. This may be characterized by $P^{[0/2]} = 1 - P^{L_1}$.
- $P^{[1/2]}$: The probability of transmitting the twin-layer HM-16QAM signals, but only L₁ is received successfully, which may be expressed as $P^{[1/2]} = P^{L_1} - P^{L_1, L_2}$.
- $P^{[2/2]}$: The probability of transmitting the twin-layer HM-16QAM signals, where both L₁ and L₂ are successfully received, which is given by $P^{[2/2]} = P^{L_1, L_2}$.
- $P^{[0/1]}$: The probability of transmitting only a single layer, namely L₁ or L₂ by using the rate-1/2 TCM 4QAM scheme, which was not received successfully. This may be characterized by $P^{[0/1]} = 1 - P^{4QAM}$.
- $P^{[1/1]}$: The probability of successfully receiving the transmitted single-layer (L₁ or L₂) information based on the rate-1/2 TCM 4QAM scheme, yielding $P^{[1/1]} = P^{4QAM}$.

Therefore, based on Section V-B, we may derive a set of single-step state-transition probabilities based on the transmit power \mathbb{P}_t of each node, as shown in Table 7, where we have $\bar{P} = 1 - P$. The notation $P_{mn}^{[i/j]}$ shown in Table 7 represents the probability of transmission from node *m* to node *n*, where *i* layers(s) was(were) successfully received out of the transmitted *j* layer(s).

D. ANALYTICAL CHARACTERIZATION

In this section, we conceived a method of analysing the attainable performance of our cooperative systems based on the single-step state-transition probability recorded in Table 7. Our theoretical analysis aims for characterizing the distribution of all possible system states, where the transition among all states is based the single-step transition probabilities defined in Table 7. The FER performance versus the transmit power \mathbb{P}_t formula is based on Eq. (7) of Section V-A, which relies on the single-step transition probabilities recorded in Table 7. The statistics used for characterizing the performance of the system are defined as follows:

- Delay_{L1} and Delay_{L2} denote the delays before the DN receives L₁ and L₂, respectively.
- $P_{outage}^{L_1}$ and $P_{outage}^{L_2}$ represent the probabilities of discarding L₁ and L₂, respectively.
- PWC denotes the average packet power consumption of the entire system.
- The notation Φ represents the average throughput of the entire system expressed in terms of packets per TS. The TS here is the time duration required for transmitting a packet containing 1,200 symbols. In order to simplify the analysis of the system, we refrain from converting each TS into actual time duration in seconds. Instead, we treat each TS as a unit in this treatise.

TABLE 7. The single-step state-transition probability table.

		TS(n+1)				
		S ₁	S ₂	S ₃	S ₄	S ₅
TS(n)	S ₁	$P_{SR_1}^{[0/2]} P_{SR_2}^{[0/2]} P_{SD}^{[0/2]}$	$P_{SR_1}^{[1/2]} P_{SR_2}^{[0/2]} P_{SD}^{[0/2]}$	$P_{SR_1}^{[2/2]} P_{SR_2}^{[0/2]} P_{SD}^{[0/2]}$	$\bar{P}_{SR_1}^{[2/2]} P_{SR_2}^{[1/2]} P_{SD}^{[0/2]}$	$P_{SR_1}^{[2/2]} P_{SR_2}^{[1/2]} P_{SD}^{[0/2]}$
	S ₂	0	$P_{R_1 R_2}^{[0/1]} P_{R_1 D}^{[0/1]}$	0	$P_{R_1 R_2}^{[1/1]} P_{R_1 D}^{[0/1]}$	0
	S ₃	0	0	$P_{R_1 R_2}^{[0/2]} P_{R_1 D}^{[0/2]}$	0	$P_{R_1 R_2}^{[1/2]} P_{R_1 D}^{[0/2]}$
	S ₄	0	0	0	$P_{R_2 D}^{[0/1]}$	0
	S ₅	0	0	0	0	$P_{R_2 D}^{[0/1]}$
	S ₆	0	0	0	0	0
	S ₇	0	0	0	0	0
	S ₈	0	0	0	0	0
	S ₉	0	0	0	0	0
	S ₁₀	0	0	0	0	0
		S ₆	S ₇	S ₈	S ₉	S ₁₀
TS(n)	S ₁	$P_{SR_2}^{[2/2]} P_{SD}^{[0/2]}$	$\bar{P}_{SR_1}^{[2/2]} P_{SR_2}^{[2/2]} P_{SD}^{[1/2]}$	$P_{SR_1}^{[2/2]} P_{SR_2}^{[2/2]} P_{SD}^{[1/2]}$	$P_{SR_2}^{[2/2]} P_{SD}^{[1/2]}$	$P_{SD}^{[2/2]}$
	S ₂	0	$P_{R_1 D}^{[1/1]}$	0	0	0
	S ₃	$P_{R_1 R_2}^{[2/2]} P_{R_1 D}^{[0/2]}$	0	$\bar{P}_{R_1 R_2}^{[2/2]} P_{R_1 D}^{[1/2]}$	$P_{R_1 R_2}^{[2/2]} P_{R_1 D}^{[1/2]}$	$P_{R_1 D}^{[2/2]}$
	S ₄	0	$P_{R_2 D}^{[1/1]}$	0	0	0
	S ₅	0	0	$P_{R_2 D}^{[1/1]}$	0	0
	S ₆	$P_{R_2 D}^{[0/2]}$	0	0	$P_{R_2 D}^{[1/2]}$	$P_{R_2 D}^{[2/2]}$
	S ₇	0	$P_{SR_1}^{[0/1]} P_{SR_2}^{[0/1]} P_{SD}^{[0/1]}$	$P_{SR_1}^{[1/1]} P_{SR_2}^{[0/1]} P_{SD}^{[0/1]}$	$P_{SR_2}^{[1/1]} P_{SD}^{[0/1]}$	$P_{SD}^{[1/1]}$
	S ₈	0	0	$P_{R_1 R_2}^{[0/1]} P_{R_1 D}^{[0/1]}$	$P_{R_1 R_2}^{[1/1]} P_{R_1 D}^{[0/1]}$	$P_{R_1 D}^{[1/1]}$
	S ₉	0	0	0	$P_{R_2 D}^{[0/1]}$	$P_{R_2 D}^{[1/1]}$
	S ₁₀	0	0	0	0	0

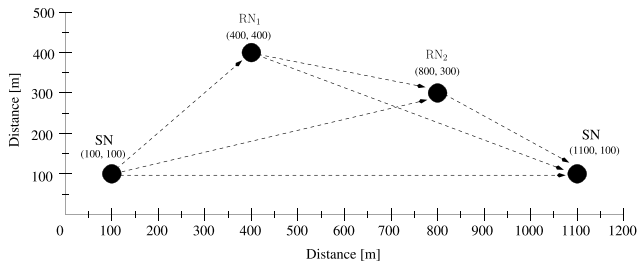


FIGURE 10. The actual hop structure of our four-node cooperative network used in theoretical analysis as well as simulations. The unit of the statistics shown in the figure is meter (m) for distance.

Note that, in this study, our system is considered to be assisted by two RNs and the channel is a Rayleigh-distributed block fading channel, where we assume that the instantaneous channel fading envelope remains unchanged throughout a single packet's transmission. In the Matlab simulations, in order to simplify the discussions, we assume that the positions of the four nodes in the cooperative network are fixed to: SN(100, 100), RN₁(400, 400), RN₂(800, 300) and DN(1100, 100) (as shown in Fig. 10), where the coordinates of the nodes are given in the round bracket. According to the 'Frontier' of L_1 and L_2 as described in Section V-B and Table 6, we are able to identify the current system state and predict the next legitimate channel state. Hence, in order to expand our four-node cooperative network to a general n -node network, we have to find the relationship among the system state S , the number of nodes in the network and the 'Frontier' of L_1 and L_2 in a given state S . Firstly, in an n -node cooperative network assisted by our twin-layer HM scheme, the number of possible system states N_{State} is $N_{State} = \frac{n(n+1)}{2}$, as seen in Eq. (8). More specifically, we may record the 'Frontier' of L_1 and L_2 in each state S in

a pair of $(N_{State} \times n)$ -element matrices, namely in S_{L1} and S_{L2} . Explicitly, the elements in these matrices can be expressed as:

$$S_{L1}(i_1, j_1) = \begin{cases} 1 & \text{if } j_1 = \left\lceil \frac{-1 + \sqrt{1 + 8i_1}}{2} \right\rceil \\ 0 & \text{else} \end{cases} \quad (9)$$

$$S_{L2}(i_2, j_2) = \begin{cases} 1 & \text{if } j_2 = i_2 - \frac{j_1(j_1 - 1)}{2} \\ 0 & \text{else,} \end{cases} \quad (10)$$

where we have $i_1 \in \{1, 2, \dots, \frac{n(n+1)}{2}\}$, $j_1, j_2 \in \{1, 2, \dots, n\}$, n is the number of nodes in the network, while $i_2 \in \{\frac{j_1(j_1-1)}{2} + 1, \dots, \frac{j_1(j_1+1)}{2}\}$. The element '1' in the matrix indicates that L_1 or L_2 appears at that node within the target state, whereas the rest of the elements will be set to '0'. Hence, when $n = 4$, the matrices S_{L1} and S_{L2} are given by:

$$S_{L1} = \begin{bmatrix} 1 & 0 & 0 & 0 \\ 0 & 1 & 0 & 0 \\ 0 & 1 & 0 & 0 \\ 0 & 0 & 1 & 0 \\ 0 & 0 & 1 & 0 \\ 0 & 0 & 1 & 0 \\ 0 & 0 & 0 & 1 \\ 0 & 0 & 0 & 1 \\ 0 & 0 & 0 & 1 \\ 0 & 0 & 0 & 1 \end{bmatrix}, \quad S_{L2} = \begin{bmatrix} 1 & 0 & 0 & 0 \\ 1 & 0 & 0 & 0 \\ 0 & 1 & 0 & 0 \\ 1 & 0 & 0 & 0 \\ 0 & 1 & 0 & 0 \\ 0 & 0 & 1 & 0 \\ 1 & 0 & 0 & 0 \\ 0 & 1 & 0 & 0 \\ 0 & 0 & 1 & 0 \\ 0 & 0 & 0 & 1 \end{bmatrix}, \quad (11)$$

where, for example, the $S_{L1}(10, 4) = 1$ indicates that at the system state S_{10} , L_1 has been successfully received at node 4 of the network, which is the DN node. Meanwhile, we define the $(N_{state} \times N_{state})$ -element single-step transition

Algorithm 1 Theoretical Analysis

```

1 while  $\text{sum}(\overline{M1}) + \text{sum}(\overline{M2}) > 10^{-6}$  do
2   if  $TS == I$  then
3      $M1(i, 1 + (Nr_{L1}(1, i) == 1)) = 1 \times Tr_{L1}(1, i)$ 
4      $M2(i, 1 + (Nr_{L2}(1, i) == 1)) = 1 \times Tr_{L2}(1, i)$ 
5   else
6     for  $i = 1:N_{state}$  do
7       for  $j = 1:N_t$  do
8         for  $k = 1:N_{state}$  do
9           %  $L_1/L_2$  broadcasted
10          if  $Nr_{L1}(i, k) == 2 / Nr_{L2}(i, k) == 2$ 
11            then
12               $M1(k, 1) = M1(k, 1) + \overline{M1}(i, j)$ 
13               $\times Tr_{L1}(i, k)$ 
14               $M2(k, 1) = M2(k, 1) + \overline{M2}(i, j)$ 
15               $\times Tr_{L2}(i, k)$ 
16            else if  $Nr_{L1}(i, k) == 1 / Nr_{L2}(i, k) == 1$ 
17            then
18               $M1(k, j+1) = M1(k, j+1)$ 
19               $+ \overline{M1}(i, j) \times Tr_{L1}(i, k)$ 
20               $M2(k, j+1) = M2(k, j+1)$ 
21               $+ \overline{M2}(i, j) \times Tr_{L2}(i, k)$ 
22            end
23            %  $L_1$  is broadcast while  $L_2$  is
24            reserved
25             $M2(k, j) = M2(k, j) +$ 
26             $\overline{M2}(i, j) \times [Tr(i, k) - Tr_{L2}(i, k)]$ 
27          end
28        end
29      end
30    end
31    % calculate delay
32    Delay $_{L1}$ (TS) = Delay1(TS)
33     $+ \sum_{i=a+1}^b \sum_{j=1}^{N_t+1} M1(i, j)$ ;
34     $M1(i, :) = 0, i \in \{a+1, \dots, b\}$ 
35    Delay $_{L2}$ (TS) = Delay2(TS)  $+ \sum_{j=1}^{N_t+1} M2(i = b, j)$ ;
36     $M2(i, :) = 0, i = b$ 
37    % calculate outage
38    Outage $_{L1}$ (TS) = out1(TS)  $+ \sum_{i=1}^b M1(i, N_t + 1)$ ;
39     $M1(i, N_t + 1) = 0, i \in \{1, \dots, b\}$ 
40    Outage $_{L2}$ (TS) = out2(TS)  $+ \sum_{i=1}^b M2(i, N_t + 1)$ ;
41     $M2(i, N_t + 1) = 0, i \in \{1, \dots, b\}$ 
42    %  $L_1$  is outage and the probability is removed
43    if  $\text{sum}(M1(i, :)) == 0$  &  $\text{sum}(M2(i, :)) \neq 0$ ,
44     $i \in \{1, \dots, a\}$  then
45      Find state  $S_k \in \{S_{a+1}, \dots, S_b\}$ , which the
46      'Frontier' of  $L_2$  is the same with that of state  $S_i$ 
47       $M2(k, :) = M2(k, :) + M2(i, :), M2(i, :) = 0$ 
48    end
49    % state appearance
50    for  $i = 1: b$  do
51      state $_{PMF}$ (i) = state $_{PMF}$ (i)
52       $+ \max(\text{sum}(M1(i, :)), \text{sum}(M2(i, :)))$ 
53    end
54     $\overline{M1} = M1$ ; clear  $M1$ 
55     $\overline{M2} = M2$ ; clear  $M2$ 
56    TS = TS + 1
57 end

```

probability matrix of the ten-state four-node system as Tr , which is recorded in Table 7. Our method is generalized in **Algorithm 1** to n nodes. In order to simplify the analysis,

the transmissions of L_1 and L_2 will be formulated separately. Therefore, a pair of flag-matrices are generated based on the matrices S_{L1} and S_{L2} , as follows:

$$Nr_{L1} = \begin{bmatrix} 1 & 2 & 2 & 2 & 2 & 2 & 2 & 2 & 2 & 2 \\ 0 & 1 & 0 & 2 & 0 & 0 & 2 & 0 & 0 & 0 \\ 0 & 0 & 1 & 0 & 2 & 2 & 0 & 2 & 2 & 2 \\ 0 & 0 & 0 & 1 & 0 & 0 & 2 & 0 & 0 & 0 \\ 0 & 0 & 0 & 0 & 1 & 0 & 0 & 2 & 0 & 0 \\ 0 & 0 & 0 & 0 & 0 & 1 & 0 & 0 & 2 & 2 \\ 0 & 0 & 0 & 0 & 0 & 0 & 0 & 0 & 0 & 0 \\ 0 & 0 & 0 & 0 & 0 & 0 & 0 & 0 & 0 & 0 \\ 0 & 0 & 0 & 0 & 0 & 0 & 0 & 0 & 0 & 0 \\ 0 & 0 & 0 & 0 & 0 & 0 & 0 & 0 & 0 & 0 \end{bmatrix}, \quad (12)$$

$$Nr_{L2} = \begin{bmatrix} 1 & 1 & 2 & 1 & 2 & 2 & 1 & 2 & 2 & 2 \\ 0 & 0 & 0 & 0 & 0 & 0 & 0 & 0 & 0 & 0 \\ 0 & 0 & 1 & 0 & 1 & 2 & 0 & 1 & 2 & 2 \\ 0 & 0 & 0 & 0 & 0 & 0 & 0 & 0 & 0 & 0 \\ 0 & 0 & 0 & 0 & 0 & 0 & 0 & 0 & 0 & 0 \\ 0 & 0 & 0 & 0 & 0 & 1 & 0 & 0 & 1 & 2 \\ 0 & 0 & 0 & 0 & 0 & 0 & 1 & 2 & 2 & 2 \\ 0 & 0 & 0 & 0 & 0 & 0 & 0 & 1 & 2 & 2 \\ 0 & 0 & 0 & 0 & 0 & 0 & 0 & 0 & 1 & 2 \\ 0 & 0 & 0 & 0 & 0 & 0 & 0 & 0 & 0 & 0 \end{bmatrix}. \quad (13)$$

These two matrices store the transmission status of the two layers. Let us consider the element $Nr_{L1}(i, j)$ for instance, where i denotes the current state and j represents the next state. When $i < 7$, $Nr_{L1}(i, j) = 0$ indicates that if the current state is S_i , the next state will not be S_j , while $Nr_{L1}(i, j) = 2$ implies that the transition from S_i to S_j is possible and the 'Frontier' of L_1 will change, whereas, $Nr_{L1}(i, i) = 1$ indicates that the 'Frontier' of L_1 will not change during the transition from S_i to S_j , where the counter of the transmission time of the current state will be increased by 1. When we have $7 \leq i \leq 10$, as mentioned in Section V-B, either L_1 will not be transmitted in the network, or it may be received by the DN or alternatively it might be discarded by the system due to exceeding the maximum number of transmission attempts N_t , which depends on the transmission time instant counters. Hence, we have $Nr_{L1}(i, j) = 0$ for $7 \leq i \leq 10$. Whilst Nr_{L2} may be deemed to be similar to Nr_{L1} by comparing Eq. (12) and Eq. (13). Note that DN may only receive L_2 in the final state S_{10} . Therefore, the single-step state transition probability matrix for L_1 can be derived as the Hadamard product of Tr and $\overline{Nr_{L1}}$, which is formulated as:

$$Tr_{L1} = Tr \circ \overline{Nr_{L1}}, \quad (14)$$

where we have:

$$\overline{Nr_{L1}}(i, j) = \begin{cases} 1 & \text{if } Nr_{L1}(i, j) = 2 \\ Nr_{L1}(i, j) & \text{if } Nr_{L1}(i, j) \neq 2. \end{cases} \quad (15)$$

Similarly, we have:

$$Tr_{L2} = Tr \circ \overline{Nr_{L2}}. \quad (16)$$

$$M1 = \begin{bmatrix} \dots & \dots \\ m1(4, 1) & m1(4, 2) & \dots & \dots & \dots & \dots & m1(4, 7) & m1(4, 8) \\ \dots & \dots \\ m1(7, 1) & \dots \\ \dots & \dots \\ m1(10, 1) & 0 & 0 & 0 & 0 & 0 & 0 & 0 \end{bmatrix} \quad (17)$$

Let us now generate a pair of $(N_{state} \times N_t + 1)$ matrices, namely $M1$ (for transmitting L_1) and $M2$ (for transmitting L_2), where the pair of matrices $M1$ and $M2$ will be used to record the transmission and re-transmission among the state-transitions. Specifically, the elements in $M1$ may be expressed as: The element $m1(k, j)$ in the matrix $M1$ indicates the probability of receiving the information L_1 when the channel state is S_k , while the transmitter in S_k embarks on making the j^{th} attempt to forward the packet L_1 . Assuming that we are at the element $m1(4, 1)$ at a random TS, this element denotes the successful transmission probability from the previous state to state S_4 . According to the transition rule defined in Fig. 9, the state S_4 may be followed by S_4 or S_7 . If we are at $m1(4, 1)$ and assume that the next transition of Fig. 9 is $S_4 \rightarrow S_4$, we may have:

$$m1(4, 2) = m1(4, 2) + m1(4, 1) \times Tr_{L1}(4, 4), \quad (18)$$

which indicates that our probability $m1(4, 1)$ will be added to $m1(4, 2)$, where $Tr_{L1}(4, 4)$ denotes the transition probability of L_1 based on the transition $S_4 \rightarrow S_4$. If reception failure occurs for six consecutive transitions, we arrive at $m1(4, 7)$, where the element '7' indicates that in state S_4 the system makes a 7th effort to forward L_1 . If the maximum number of attempts at each node is $N_t = 7$, then $m1(4, 7)$ may only have a single final transition. If successful, then we may have:

$$m1(7, 1) = m1(7, 1) + m1(4, 7) \times Tr_{L1}(4, 7), \quad (19)$$

implying that the probability $m1(4, 7)$ will be added to $m1(7, 1)$ for the next transition. However, if the transition fails again, we arrive at:

$$m1(4, 8) = m1(4, 8) + m1(4, 7) \times Tr_{L1}(4, 4), \quad (20)$$

noting that we have $N_t = 7$, while $m1(4, 8)$ represents the failure probability of the 7th attempt of S_4 traversing from $m1(4, 1)$ to $m1(4, 8)$. Hence, the probability $m1(4, 8)$ should now be removed from the matrix $M1$, since no more attempts are available for S_4 . Note that $m1(10, 1)$ represents the probability that DN successfully received both L_1 and L_2 during the current TS. The processing procedure of the probability matrix $M2$ for the transitions of L_2 is similar to that of L_1 , but it is based on the single-transition probability matrix Tr_{L2} . Our theoretical analysis based on $M1$ and $M2$ is detailed in **Algorithm 1**, whilst the corresponding simplified flow-chart based on **Algorithm 1** is illustrated in Fig. 11.

Again, for $j = N_t + 1$, the related transmission of L_1 or L_2 will be abandoned and the 'Outage' counter will be incremented. In **Algorithm 1**, we have $a = \frac{n(n-1)}{2}$

and $b = \frac{n(n+1)}{2}$, where n is the number of nodes in the cooperative network. Note that when the system's state is S_i ($i \leq a$), the system does not receive any information. Meanwhile, during the state-transition from $S_{(a+1)}$ to $S_{(b-1)}$, only L_1 of the twin-layer HM scheme is received successfully by the DN. The final state S_b indicates that both L_1 and L_2 have been successfully transmitted to DN.

The specific segment of **Algorithm 1** spanning from line 2 to 22 calculates the probabilities of all the possible state-transitions of the current TS based on the previous probability matrix $\overline{M1}$ as well as $\overline{M2}$, and the results are recorded in $M1$ and $M2$ as shown by line 3 to 4 of **Algorithm 1**. Note that, during the first TS, we set the probability of successfully receiving L_1 and L_2 to '1'. The segment of **Algorithm 1** spanning from line 23-27 is to calculate the number of TSs that the DN needs for receiving L_1 and L_2 , which determines the associated normalized delay. We also mention that, every time we derive $Delay_{L1}$ and $Delay_{L2}$ of the current TS, we have to clear the elements in $M1$ and $M2$ which were used during the calculations, because these probabilities are assumed to represent the information that the DN has successfully received a packet. Hence, they should not remain in the matrix for the ensuing calculations of **Algorithm 1**. The segment of **Algorithm 1** ranging from 28-32 is to calculate the outage probabilities of L_1 and L_2 of the current TS. As we mentioned before, the element in $M1(i, j)$ represents the probability of the state S_i associated with transmitting L_1 for the j^{th} time. Therefore, all the elements in $M1(i, j)$ associated with $j = N_t + 1$ and $i \leq a$ represent the outage probability of L_1 during the current TS. Since the elements involved in the $Delay_{L1}$ calculations have been cleared, we may derive the outage probability of L_1 during the current TS, as shown in line 29. As for receiving L_2 , since the DN may only receive L_2 in the system state S_b , all the elements in $M2(i, j)$ associated with $j = N_t + 1$ and $i \leq b - 1$ may be considered to represent the outage probability of L_2 . Note that since the elements involved in the $Delay_{L2}$ calculations have also been cleared, the outage probability of L_2 during the current TS may be derived as in line 31 of **Algorithm 1**. Similar by to the delay calculations, the matrix elements $M1$ and $M2$ involved in the outage probability calculations should also be cleared, because in cooperative communications this part of the information will be discarded by the system, when the transmission attempt counter exceeds N_t . Hence, the specific elements in $M1$ and $M2$, which are involved in the outage probability calculations should not remain in the matrix for the calculations during the next TS.

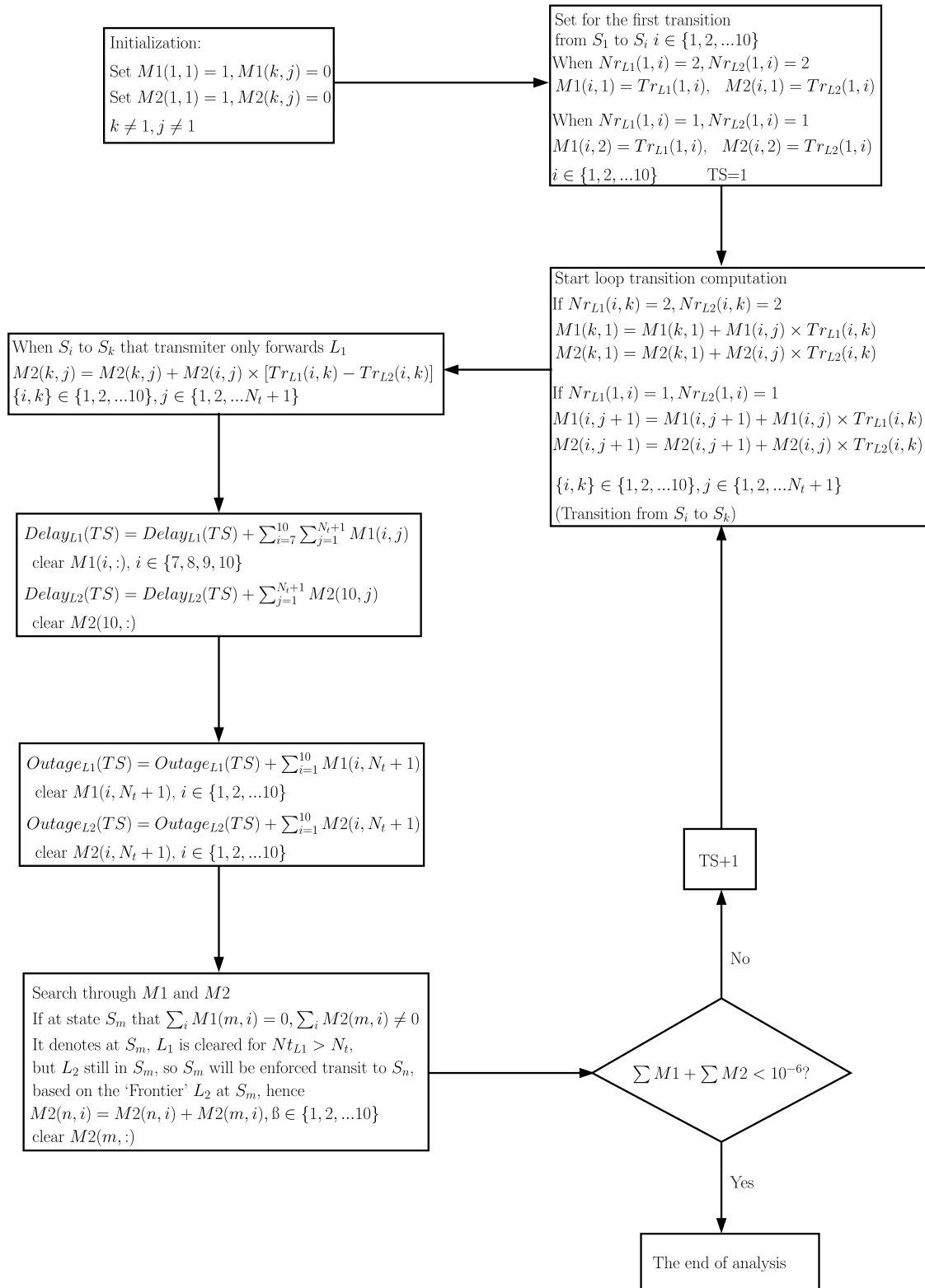


FIGURE 11. The flow-chart of the theoretical analysis of our HMOR algorithm aided four-node cooperative network of Fig. 10. The flow-chart is based on Algorithm 1, where the related simulation parameters are listed in Table 4 and the system's schematic is described in Section V-B.

Additionally, when L_1 is discarded by the system, since the transmission attempt counter at the target transmitter exceeds N_t , the current state S_i will be forced to traverse

to S_k , where $k \in \{a + 1, \dots, b\}$, if the 'Frontier' of L_2 at state S_k is the same as that at state S_i . Hence, all the elements in $M2(i, :)$ should be copied to $M2(k, :)$, while the elements

in $M2(i, :)$ should be cleared after this copying process, as shown in Line 33-37 of **Algorithm 1**. The probabilities of encountering the specific number of appearances for each state are computed in the segment of **Algorithm 1** spanning from line 38-41. Additionally, the segment ranging from Line 42-44 represents populating the ‘new previous probability matrix’ $\overline{M1}$ as well as $M2$ and clearing $M1$ and $M2$ for the next TS. Note that the loop of **Algorithm 1** is controlled by the total probabilities of remaining in $\overline{M1}$ and $M2$. When we have $\text{sum}(\overline{M1}) + \text{sum}(M2) < 10^{-6}$, we assumed that the twin-layer information is successfully received by the DN, hence the loop will be terminated. Therefore, we may normalise the distribution of $Delay_{L1}$ and $Delay_{L2}$ as follows:

$$Delay_{L1}(i) = \frac{Delay_{L1}(i)}{\sum Delay_{L1}(i)}, \quad (21)$$

$$Delay_{L2}(j) = \frac{Delay_{L1}(j)}{\sum Delay_{L2}(j)}, \quad (22)$$

which are also known as the Probability Mass Function (PMF). According to $Delay_{L1}$ and $Delay_{L2}$, the Cumulative Distribution Function (CDF) of the delay of L_1 and L_2 may be expressed as:

$$CDF_{L1}(k) = \sum_k^{i=1} Delay_{L1}(i), \quad (23)$$

$$CDF_{L2}(k) = \sum_k^{i=1} Delay_{L2}(i). \quad (24)$$

Furthermore, the outage probability of L_1 and L_2 may be formulated as:

$$P_{outage}^{L1} = \sum Outage_{L1}(i), \quad (25)$$

$$P_{outage}^{L2} = \sum Outage_{L2}(j). \quad (26)$$

Hence, the throughput of the entire system may be characterized as:

$$\Phi = \frac{2 - P_{outage}^{L1} - P_{outage}^{L2}}{\sum state_{PMF}}, \quad (27)$$

where, the $state_{PMF}$ records the appearance of each state throughout the entire transmission process. Meanwhile, in the analysis, instead of assuming that all the nodes in the network has the same transmit power, we are going to find the optimized \mathbb{P}_t for each node. Based on the discussions of Section V-B, at each system state, the transmitter node is given. Explicitly, the node index χ of the transmitter in the n -node network may be inferred from the current state index i as follows:

$$\chi = \begin{cases} \left\lceil \frac{-1 + \sqrt{1 + 8i}}{2} \right\rceil & \text{if } 1 \leq i \leq \frac{n(n-1)}{2} \\ i - \frac{n(n-1)}{2} & \text{if } \frac{n(n-1)}{2} + 1 \leq i \leq \frac{n(n+1)}{2}. \end{cases} \quad (28)$$

Therefore, the total power consumption E_{total} may be expressed as:

$$E_{total} = \sum_{i=1}^{N_{state}} state_{PMF}(i) \times \mathbb{P}_t(\chi). \quad (29)$$

Hence, the average power consumption (\overline{PWC}) per packet may be formulated as:

$$\overline{PWC} = \frac{E_{total}}{2 - P_{outage}^{L1} - P_{outage}^{L2}}. \quad (30)$$

It may be observed that, \overline{PWC} is jointly determined both by E_{total} as well as by outage probabilities P_{outage}^{L1} and P_{outage}^{L2} . During the analysis, our results were generated according to the specific value of N_t . At a specific value of N_t , we have set the \mathbb{P}_t in the range spanning from $10^{-6} W$ to $0.1 W$ at all the three nodes in the network, namely at SN, RN_1 and RN_2 , for the sake of finding the optimum \mathbb{P}_t for each node for arriving at the minimum per-packet power consumption of \overline{PWC} . The search procedure conducted in two rounds. Firstly, we initialise all the nodes to a low power of $\mathbb{P}_t = 10^{-3} W$ and commence the search from RN_2 , namely the node nearest to DN, and then moving backwards to SN. After the first round of the search, we may arrive at the optimized \mathbb{P}_{tSN}^1 , \mathbb{P}_{tRN1}^1 and \mathbb{P}_{tRN2}^1 . All these three values will be the initial values for round two. Then the search process will be repeated for another round. Therefore, we may find the optimized value of \mathbb{P}_{tSN} , \mathbb{P}_{tRN1} and \mathbb{P}_{tRN2} for deriving the minimum per-packet power consumption of \overline{PWC} . The \mathbb{P}_{tSN} , \mathbb{P}_{tRN1} and \mathbb{P}_{tRN2} values derived during the theoretical analysis will also be employed in the simulations for checking whether the results of our theoretical method match the simulation results. In order to provide fair comparisons between our scheme and the TOR scheme, all the results of Section VII will be based on the optimized per-packet power \overline{PWC} .

VI. SYSTEM SIMULATIONS

The flow chart of the simulation for the single packet's transmission is illustrated in Fig. 12, which is detailed in the **Algorithm 2**. **Algorithm 2** illustrates the schedule of our simulations in the context of the cooperative communication system considered. To be more specific, the number of sample-packet transmitted is set to $N_{ST} = 10^5$. As discussed in Section V-B, for every specific state of Table 6, the twin-layer information stream of L_1 and L_2 will have reached a specific position in the cooperative networks. Given the current state, according to the transmission rule defined in Fig. 9 of Section V-B, we activate the corresponding transmission for the following TS. Then, based on the FER versus SNR performance characterized in Section V-A, the success or failure status of L_1 and L_2 during the current transmission may be evaluated. When deciding whether the node is capable of successfully receiving the packet or not, we will generate a random variable $v \in u(0, 1)$, where $u(0, 1)$ represent the uniform distribution within the range $[0, 1]$. Explicitly, if we

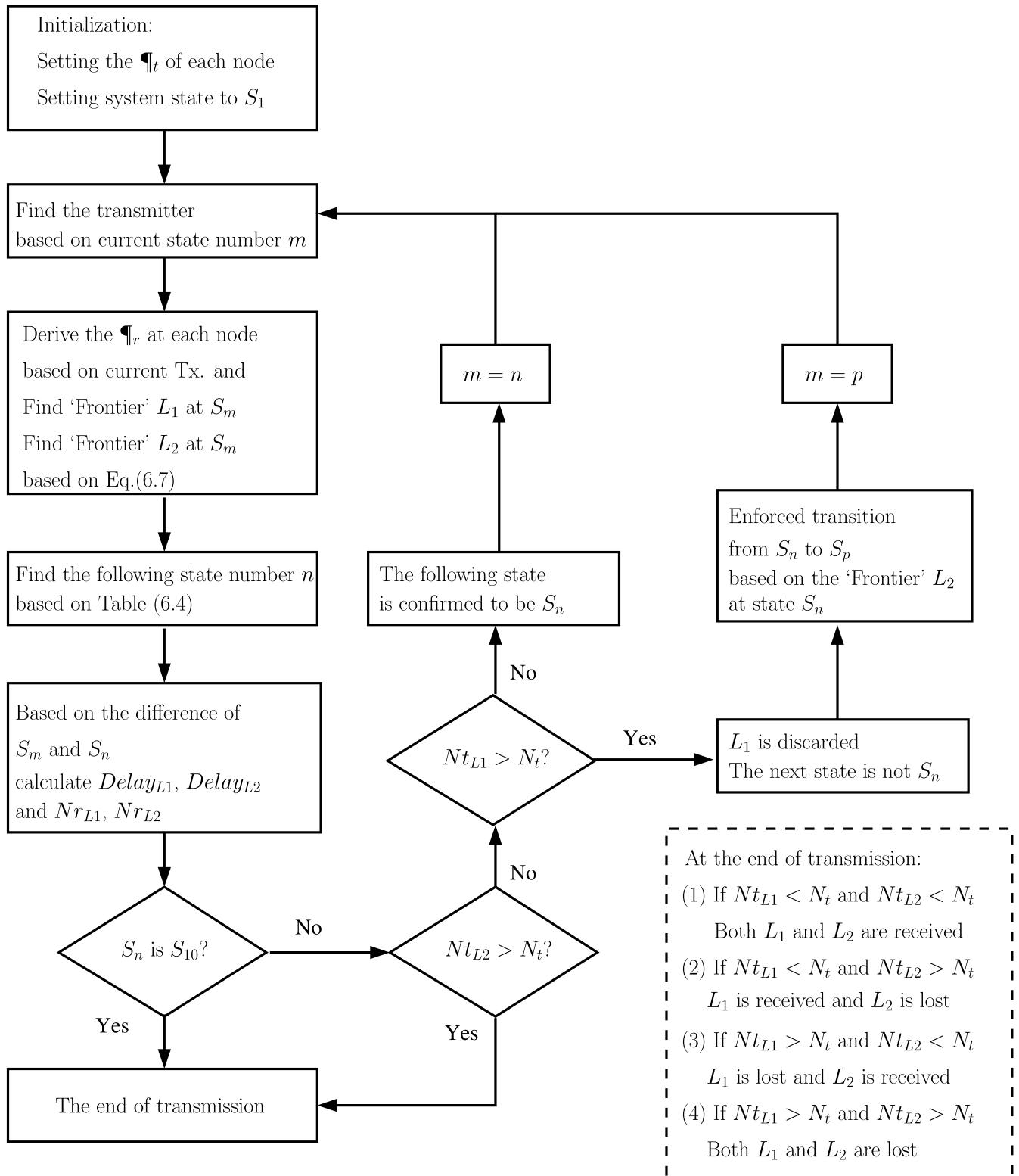


FIGURE 12. The flow-chart of a single packet's transmission in our HMOR algorithm aided four-node cooperative network of Fig. 10. The flow-chart is based on Algorithm 2, where the related simulation parameters are listed in Table 4 and the system's schematic is described in Section V-B.

have $\nu \leq FER_{target}$, the status of the target node would be considered to be 'failed'. By contrast, if $\nu > FER_{target}$, the transmission between the transmitter and the target node would be successful. Therefore, once we identified the

transmission success/failure status based on the current state, the next state to be encountered by our transmissions regime may be predicted, as shown in the segment spanning from line 4 to 8 in Algorithm 2.

Algorithm 2 System Simulation

```

1  for  $i=1$ :simulation-time do
2      current state  $S_{current} = S_1$ 
3      while Brake-flag==0 do
4          Generate channel fading based on  $S_{current}$ .
5          Derive the instantaneous SNR at each node
           based on current transmitter. Then, find the
           correspond FER of receiving  $L_1$  and  $L_2$  at
           each receiver candidate.
6          Judging the next state  $S_{next}$  based on
           Section V-A and V-B
7          Setting up the new transmitter.
8          % calculate delay
9          if  $S_{next} > S_a \& S_{current} \leq S_a$  then
10             Delay $_{L_1}$ (TS)=Delay $_{L_1}$ (TS)+1
11         end
12         if  $S_{next} = S_{10}$  then
13             Delay $_{L_2}$ (TS)=Delay $_{L_2}$ (TS)+1
14         end
15         % record the times each states appeared
16         State(state $_{num}$ ) = State(state $_{num}$ ) + 1
17         % calculate transmission time
18         if Frontier of  $L_1$  unchanged & transmitter is
           forwarding  $L_1$  then
19              $N_{tL_1} = N_{tL_1} + 1$ 
20         else
21              $N_{tL_1} = 1$ 
22         end
23         if Frontier of  $L_2$  unchanged & transmitter is
           forwarding  $L_2$  then
24              $N_{tL_2} = N_{tL_2} + 1$ 
25         else if Frontier of  $L_2$  unchanged &
           transmitter is not forwarding  $L_2$  then
26              $N_{tL_2} = N_{tL_2}$ 
27         else
28              $N_{tL_2} = 1$ 
29         end
30         % calculate outage
31         if  $N_{tL_2} > N_t \& out_{L_2} == 0$  then
32              $out_{L_2count} = out_{L_2count} + 1$ 
33              $out_{L_2} = 1$ 
34         end
35         if  $N_{tL_1} > N_t \& S_{next} \leq S_a$  then
36              $out_{L_1count} = out_{L_1count} + 1$ 
37             Forcing the  $S_{next}$  to transfer to
              $S_{next} \in \{S_{(a+1)}, S_{(a+2)}, \dots, S_{(b-1)}\}$  based
             on the current position of  $L_2$  (shown in
             Section V-B).
38         end
39         % end the loop
40         if  $S_{current} = S_b$  then
41             Brake-flag=1; break
42         end
43         if  $S_a < S_{current} < S_b \& out_{L_2} == 1$  then
44             Brake-flag=1; break
45         end
46          $S_{current} = S_{next}$ 
47         TS = TS+1
48     end
49 end

```

The segment ranging from line 8 to 14 records the number of TSs the L_1 and L_2 streams required to be conveyed to the DN. Furthermore, line 16 of **Algorithm 2** records the

number of events that each state occurred during the entire transmission process, which will be used for calculating the power consumption of the entire system. The segment ranging from line 17 to 29 of **Algorithm 2** counters the retransmission attempts at the current transmitter. If the ‘Frontier’ of L_1 remains unchanged, the value of the counter N_{rL_1} will be incremented by one, otherwise, the N_{rL_1} counter will be set to one. If the ‘Frontier’ of L_2 remains unchanged and the transmitter is transmitting L_2 , the value of N_{rL_2} will be incremented by one. However, if the ‘Frontier’ of L_2 remains unchanged, but the transmitter is not going to transmit L_2 during the following TS, the value of N_{rL_2} will be kept unchanged, otherwise, the N_{rL_2} counter will be set to one. Recall that, the decision concerning the transmitter’s specific action and the particular choice of information that the transmitter is going to forward during the next TS were defined in Section V-B. The segment spanning from line 30 to 38 is included in order to decide, whether the system has to discard any information. When we have $N_{rL_2} > N_r$, the system will discard L_2 , the transmission attempt counter out_{L_2count} will be incremented by one, and the flag out_{L_2} will be reset to one. As for N_{rL_1} , if it exceeds the maximum tolerable number of transmission attempts N_t , while the DN still does not receive anything ($S_{next} \leq S_a$), then the new state will have to obey $S_{next} \in \{S_{(a+1)}, S_{(a+2)}, \dots, S_{(b-1)}\}$, which depends on the ‘Frontier’ of L_2 . Note that in this situation, the actions of **Algorithm 2** in the segment spanning from line 8 to 11 will not be activated during the next loop. Hence, L_1 will be discarded when the entire loop ends. Furthermore, lines 39 to 45 are related to testing the conditions under which to terminate the loop. Finally, lines 46-47 update the system’s state and increment the TS counter for the next loop.

Whist the calculation of the system characteristics carried out during the simulations is different from that in the theoretical analysis, the distributions of $Delay_{L_1}$ and $Delay_{L_2}$ are the same as those in Eq. (21) and Eq. (22), respectively. By the same token, CDF_{L_1} and CDF_{L_2} are also the same as those in Eq. (23) and Eq. (24). The simulation-based outage probability of L_1 and L_2 is given by:

$$P_{outage}^{L1} = \frac{out_{L_1count}}{N_{ST}}, \quad (31)$$

$$P_{outage}^{L2} = \frac{out_{L_2count}}{N_{ST}}, \quad (32)$$

which are different from those in Eq. 25 and Eq. 26, where again, the total number of packets simulated $N_{ST} = 10^5$. Therefore, the throughput of the system may be expressed as:

$$\Phi = \frac{2 \times N_{ST} - out_{L_1count} - out_{L_2count}}{TS_{total}}, \quad (33)$$

where the total power consumption ‘ E_{total} ’ while transmitting N_{ST} packets is the same as that defined in (29). The simulation-based average packet-power consumption \overline{PWC} may be formulated as:

$$\overline{PWC} = \frac{E_{total}}{(2 - P_{outage}^{L1} - P_{outage}^{L2}) \times N_{ST}}. \quad (34)$$

VII. PERFORMANCE ANALYSIS

In this section, we first compared our twin-layer TTCHM-16QAM aided OR scheme to the TOR scheme. Furthermore, we also compared the performance of a four-node network to a ten-node network, both of them employing our cooperative communication protocol described in Section V-B. Note that in order to make a fair comparison of the systems, the transmit power \mathcal{P}_t of each node has been optimized for achieving the minimum \overline{PWC} for the given value of N_t .

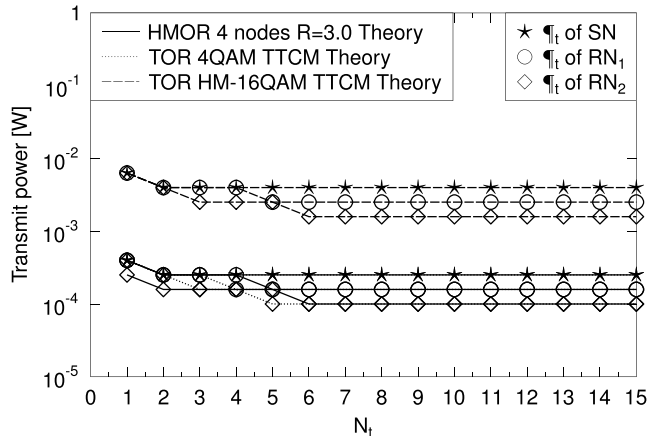


FIGURE 13. The optimized power \mathcal{P}_t of the SN, RN_1 and RN_2 versus the maximum number of transmission attempts N_t of the four-node cooperative communication network considered. The related simulation parameters are listed in Table 4, while the system’s schematic is described in Section V-B and the network’s topology is seen in Fig. 10.

A. COMPARISON TO TRADITIONAL OPPORTUNISTIC ROUTING

The TOR scheme has been lavish by document, for example in [81] and [94]. Fig. 13 represents the optimized \mathcal{P}_t of each single node in the four-node cooperative network. It may be observed from Fig. 13 that upon increasing N_t , the optimized power \mathcal{P}_t exhibits a slight reduction tendency upto $N_t = 6$, but for $N_t > 6$, it will remain near-constant. Recall that in our cooperative communication protocol, the TTCM aided twin-layer HM-16QAM packet may become partitioned during its transmission. Hence, the optimized power \mathcal{P}_t of each single node of our HMOR scheme is the same as those of the TOR scheme transmitting TTCM coded 4QAM signal packets. Consider $N_t = 7$ for instance, where the optimized power \mathcal{P}_t of each node of our twin-layer HM-16QAM OR and of the TTCM coded 4QAM TOR are: $\mathcal{P}_{tSN} = 0.2512$ mW, $\mathcal{P}_{tRN1} = 0.1585$ mW and $\mathcal{P}_{tRN2} = 0.1$ mW. However, when using the TOR scheme to transmit the TTCM aided twin-layer HM-16QAM packets, we have higher transmit power values, namely, $\mathcal{P}_{tSN} = 3.98$ mW, $\mathcal{P}_{tRN1} = 2.51$ mW and $\mathcal{P}_{tRN2} = 1.58$ mW, when $N_t = 7$. Therefore, Fig. 13 indicates that, the HMOR scheme is capable of substantially reducing the power \mathcal{P}_t of each single node in the network.

The optimized per-packet power consumption \overline{PWC} of the four-node cooperative communication network is shown

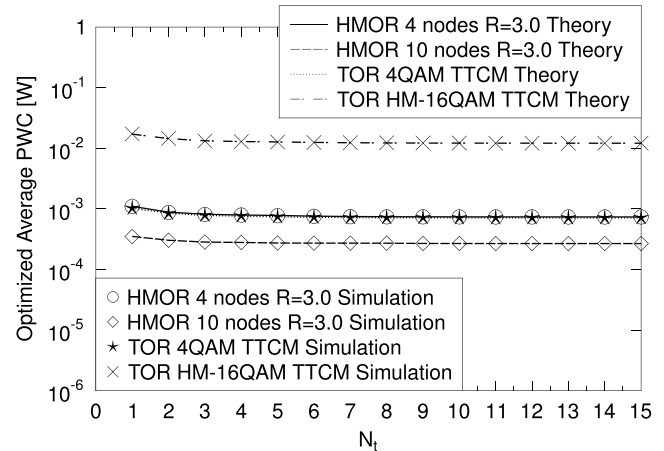


FIGURE 14. The optimized average per-packet power-consumption \overline{PWC} versus the maximum number of transmission attempts N_t of our four-node cooperative communication network. The related simulation parameters are listed in Table 4, while the system’s schematic is described in Section V-B and the network’s topology is seen in Fig. 10.

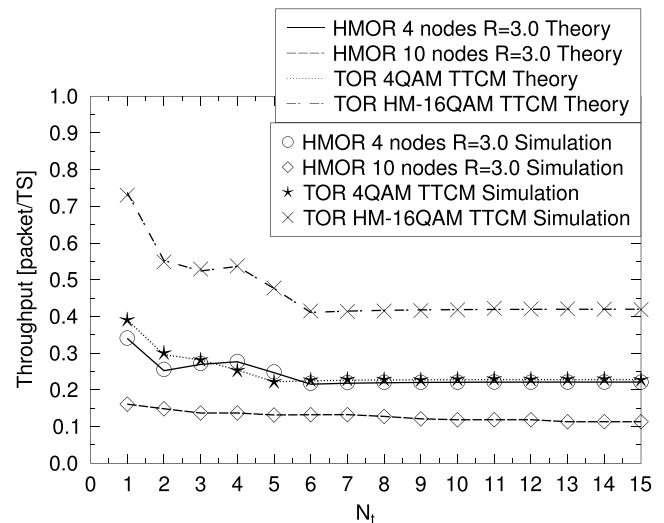


FIGURE 15. The throughput versus the maximum number of transmission attempts N_t of four-node cooperative communication network. The related simulation parameters are listed in Table 4, while the system’s schematic is described in Section V-B and the network’s topology is seen in Fig. 10.

in Fig. 14. The curves seen in Fig. 14 show the minimum \overline{PWC} that the specific OR scheme may achieve for a given number of transmission attempts of N_t . It may be observed that, for $N_t = 7$, the minimized \overline{PWC} of our four-node based TTCM aided twin-layer HM-16QAM scheme becomes $\overline{PWC}_{min} \approx 0.74$ mW, while \overline{PWC}_{min} of the TOR transmitting TTCM aided 4QAM packets is only slightly lower than that of HMOR scheme, which is about 0.71 mW. However, for $N_t = 7$, the minimum \overline{PWC} that the TOR scheme transmitting TTCM aided HM-16QAM packets may achieve is 12.37 mW.

The throughput of the four-node cooperative network of Fig. 10 is represented in Fig. 15. The simulation results are

TABLE 8. The simulation results summarized from Fig. 13 to Fig. 15. The related simulation parameters are listed in Table 4, while the system’s schematic is described in Section V-B and the network’s topology is seen in Fig. 10.

Code	TTCM				
Modulation	4QAM, HM-16QAM				
N_t	7				
Positions of the nodes	SN(100,100), RN ₁ (400,400), RN ₂ (800,300), DN(1000,100)				
	\mathcal{P}_t^{SN} mw	$\mathcal{P}_t^{RN_1}$ mw	$\mathcal{P}_t^{RN_2}$ mw	Opt. \overline{PWC} mw	Φ [packet/TS]
HMOR	0.2512	0.1585	0.1000	0.7423	0.2200
TOR 4QAM	0.2512	0.1585	0.1000	0.7133	0.2279
TOR HM-16QAM	3.981	2.512	1.585	12.365	0.4136

based on the statistics illustrated in Fig. 13 and Fig. 14. As expected upon increasing N_t , the throughput of all the schemes is reduced. Based on the minimized average per-packet power-consumption \overline{PWC} and optimized power \mathcal{P}_t of every node in the network, the throughput of our HMOR scheme becomes similar to that of the TOR scheme transmitting TTCM coded 4QAM packets, which is $\Phi \approx 0.22$ [packet/TS] for $N_t = 7$. By contrast, the throughput Φ of the TOR scheme transmitting TTCM aided twin-layer HM-16QAM packets is about 0.41 [packet/TS] for $N_t = 7$. However, the price we paid for the increased throughput is an about ten times higher power \mathcal{P}_t at each single node of the entire network, as shown in Fig. 13. Note that, if we set $\mathcal{P}_t^{SN} = 3.98$ mW, $\mathcal{P}_t^{RN_1} = 2.51$ mW and $\mathcal{P}_t^{RN_2} = 1.58$ mW, the throughput of our HMOR scheme transmitting TTCM aided twin-layer HM-16QAM packets will be increased to 0.894 [packet/TS]. In a nutshell, we focussed our attention on the attainable system performance for $N_t = 7$, where the related results portrayed in Fig. 13 to Fig. 15 are summarized in Table 8.

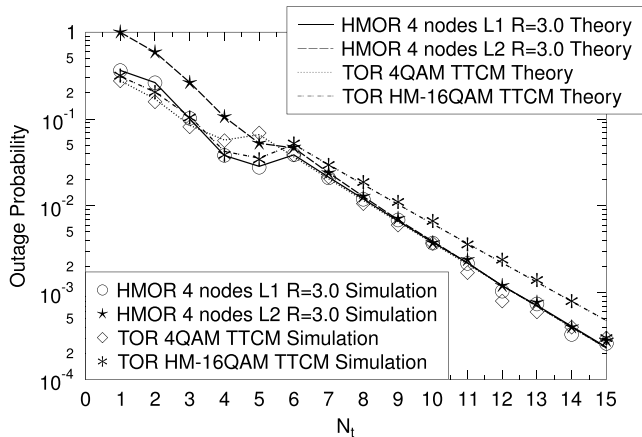


FIGURE 16. The outage probability versus the number of maximum transmission attempts of each node N_t based on different OR schemes. The statistics are all based on the minimized \overline{PWC} for each scheme at a given value of N_t . The related simulation parameters are listed in Table 4, while the system’s schematic is described in Section V-B and the network’s topology is seen in Fig. 10.

Fig. 16 illustrates the outage probability P_{outage} of both our HMOR scheme and that of the TOR scheme. Since HMOR scheme may partition the TTCM aided twin-layer HM-16QAM signal into two packets during its transmission, we have to define a pair of outage probabilities namely

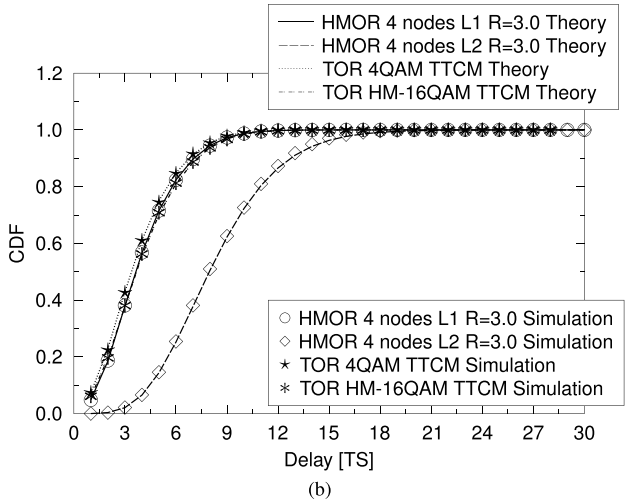
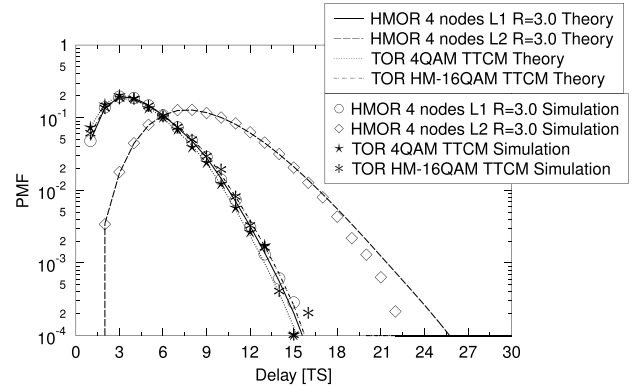


FIGURE 17. The PMF and the CDF of the four-node cooperative network’s delay based on different OR schemes. The statistics are all based on the minimized \overline{PWC} for each scheme given $N_t = 7$. The related simulation parameters are listed in Table 4, while the system’s schematic is described in Section V-B and the network’s topology is seen in Fig. 10. (a) PMF of the delay for $N_t = 7$. (b) CDF of the delay for $N_t = 7$.

P_{outage}^{L1} and P_{outage}^{L2} . It may be observed that upon increasing the number of transmission attempts N_t , the outage probabilities of all the three schemes characterized in Fig. 16 will be reduced. Based on their minimized per-packet power-consumption \overline{PWC} , when considering $N_t > 6$, the outage probabilities of both L_1 and L_2 of our twin-layer OR scheme, as well as that of the TOR transmitting TTCM aided twin-layer HM-16QAM packets that of the TOR transmitting single layer TTCM coded 4QAM packets becomes similar. Fig. 17(a) illustrate the PMF of our HMOR scheme’s delay

for $N_t = 7$. By contrast, the CDF of our HMOR scheme's delay and that of the TOR scheme is represented in Fig. 17(b) for $N_t = 7$. Again, all the results shown in Fig. 17(b) are based on the minimized \overline{PWC} for each specific OR scheme. It may be observed that the CDF of $Delay_{L_1}$ of our twin-layer OR scheme is similar to that of the two traditional schemes. Quantitatively, 99.5% of the packets may be received with a delay of 11 TSs or less. But as shown in Fig. 13, Fig. 14 and Fig. 15, in order to transmit the TTCM coded twin-layer HM-16QAM packets at a lower \overline{PWC} as well as at a lower \mathcal{P}_t of each node in the network, the price paid by our HMOR scheme is the extended delay of receiving L_2 of the twin-layer HM-16QAM packets at DN. Explicitly, 96.3% of L_2 of the twin-layer HM-16QAM packets may be received with a delay of 15 TSs or less.

the four-node cooperative wireless *ad hoc* network shown in Fig. 10. The maximum number of transmission attempts for each node of the cooperative network is set to $N_t = 7$. Note that the power \mathcal{P}_t of each node of the HMOR algorithm associated with the HM ratio of $R_1 = 3.0$ is similar to that of the TOR algorithm transmitting 4QAM TTCM packets. It may be observed in Fig. 18(b) that 97.7% of the second packet of the TOR algorithm transmitting 4QAM TTCM coded packets will be received with a maximum delay of 15 TSs. This is similar to that of $Delay_{L_2}$ of our HMOR algorithm associated with the HM ratio of $R_1 = 3.0$. The related results are summarized in Table 9.

TABLE 9. The summarized simulation results from Fig. 16 to Fig. 18. The related simulation parameters are listed in Table 4, while the system's schematic is described in Section V-B and the network's topology is seen in Fig. 10.

Code	TTCM	
N_t	7	
Constraints on Delay	95% plus of packets received	
Constraints on \mathcal{P}_t	The \overline{PWC} of all schemes are minimized	
	Outage P_{outage}	Delay (TS)
HMOR L_1	0.0210	9 (97.33%)
HMOR L_2	0.0239	15 (97.04%)
TOR 4QAM	0.0215	8 (95.36%)
TOR 4QAM (two packets)	–	15 (97.66%)
TOR HM-16QAM	0.0296	9 (96.67%)

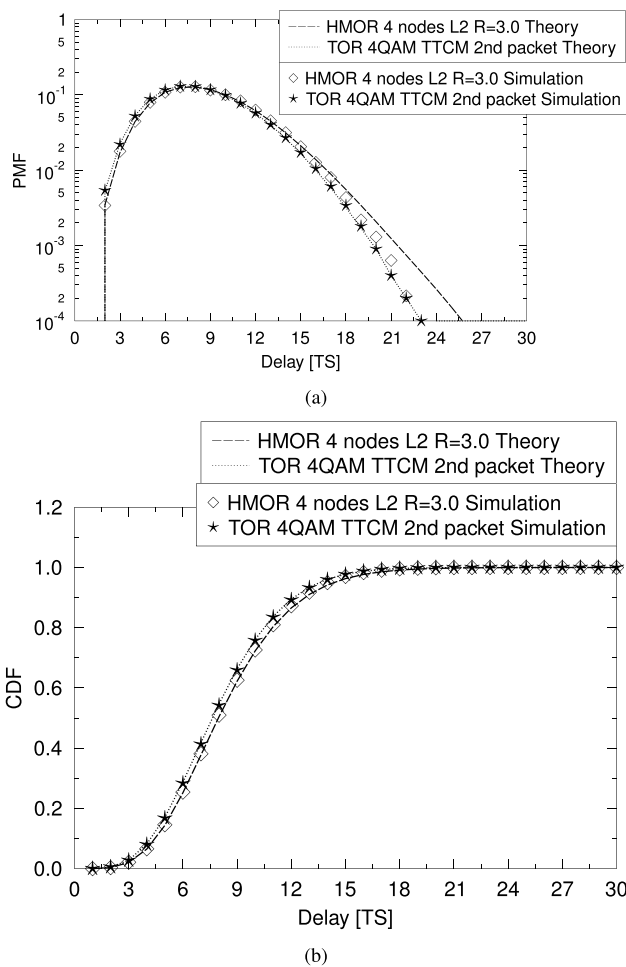


FIGURE 18. The PMF and the CDF of the four-node cooperative network's delay based on different OR schemes. The statistics are all based on the minimized \overline{PWC} for each scheme given $N_t = 7$. The related simulation parameters are listed in Table 4, while the system's schematic is described in Section V-B and the network's topology is seen in Fig. 10. (a) PMF of the delay for $N_t = 7$. (b) CDF of the delay for $N_t = 7$.

Fig. 18 illustrates our comparison between the TOR algorithm during receiving two packets and of the HMOR algorithm receiving L_2 . The system considered is

Additionally, in Fig. 13 to Fig. 18, the legend 'Theory' indicates that the results based on our theoretical analysis in **Algorithm 1**, while the legend 'Simulation' indicates that the results are from simulation method outlined in **Algorithm 2**. According to the above figures, it can be observed that our simulation results based on **Algorithm 2** closely match the theoretical results of **Algorithm 1**, which confirm each other.

B. INCREASING THE NETWORK SIZE

In Fig. 14 and Fig. 15, we have also presented the performance of a ten-node cooperative network consisting of eight RNs using our HMOR scheme for transmitting TTCM-coded twin-layer HM-16QAM packets. The position of the nodes as well as the related optimized power \mathcal{P}_t ($N_t = 7$) is shown in Table 10. Note that the positions of the RN nodes are uniformly distributed between the SN to DN node.

It can be observed from Fig. 14 that the minimized per-packet power consumption \overline{PWC} of the ten-node network using our HMOR scheme for transmitting twin-layer HM-16QAM packets is even lower than that of the four-node network using the same communication protocol, which is $\overline{PWC} = 0.271$ mW. When the number of relays in the network that was activated for assisting the transmissions is increased, the power \mathcal{P}_t may be reduced as a benefit of the lower distance between the neighbouring nodes. Note that in the ten-node network of Fig. 19, the eight RNs are uniformly placed between the SN to DN link. However, Fig. 15 shows that based on the minimized per-packet power consumption \overline{PWC} associated with a specific N_t , the throughput of the

TABLE 10. The table of the node positions and the related optimized transmission power \mathcal{P}_t of the ten-node cooperative networks. The related simulation parameters are listed in Table 4, while the system's schematic is described in Section V-B and the network's topology is seen in Fig. 19.

Nodes	Position [m]	\mathcal{P}_t [mw]
SN	(100, 100)	0.010
RN ₁	(216.9, 98.6)	0.100
RN ₂	(292.8, 250.3)	0.100
RN ₃	(606.7, 7.5)	0.040
RN ₄	(622.0, 149.8)	0.063
RN ₅	(821.4, -355.1)	0.016
RN ₆	(885.3, -407.6)	0.025
RN ₇	(953.4, 110.7)	0.010
RN ₈	(995.1, 74.6)	0.016
DN	(1100, 100)	-

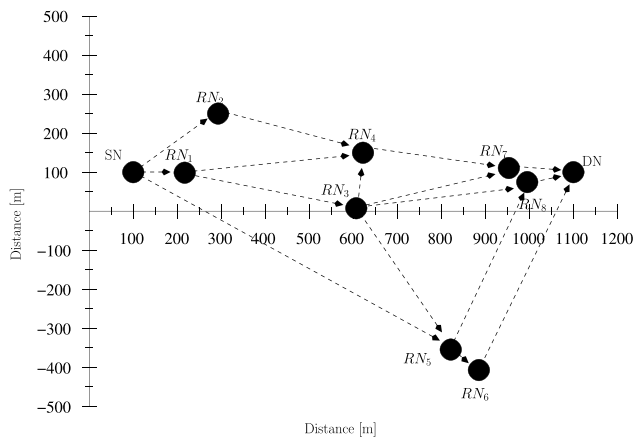


FIGURE 19. The actual hop structure of our ten-node cooperative network used in the theoretical analysis as well as in the simulations. The unit of the distance shown in the figure is meter (m). The positions of the nodes are shown in Table 10.

ten-node network using our HMOR scheme also becomes lower than that of the four-node network, which is about $\Phi \approx 0.132$ [packet/TS] for $N_t = 7$.

Fig. 20 indicates that based on the minimized per-packet power consumption \overline{PWC} and for a specific $N_t < 7$, the outage probabilities P_{outage}^{L1} and P_{outage}^{L2} of the ten-node system are consistently higher than those of the four-node system. By contrast, for higher N_t values their outage probabilities are similar to each other. The reason for this trend is that the optimized power \mathcal{P}_t of the ten-node system becomes even lower than that of the four-node system. However, the reduced power \mathcal{P}_t increases the outage probabilities, especially for L_2 . Nonetheless, having a sufficiently high number of maximum transmission attempts N_t , the outage probability can indeed be reduced. Fig. 21(a) and Fig. 21(b) compares the PMF and the CDF of both $Delay_{L1}$ and $Delay_{L2}$ of the ten-node system to that of the four-node system, when both of the systems operate at \overline{PWC} minimized according to $N_t = 7$. It may be observed that when the number of nodes in the network is increased, and minimized per-packet power consumption \overline{PWC} is used for the entire system, this typically increases the delay of the DN receiving L_1 and L_2 of the twin-layer HM-16QAM packets scheme. When $N_t = 7$, 96.9% of the

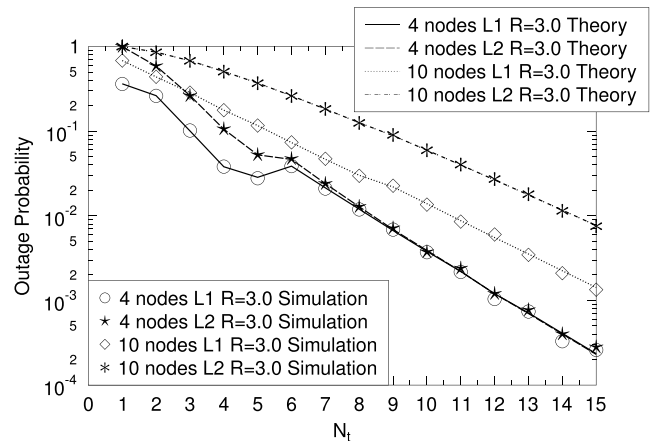


FIGURE 20. The outage probability of the cooperative network based on our HMOR schemes versus the maximum transmission attempts N_t . TCM aided HM-16QAM signals are transmitted and the HM ratio is $R_1 = 3.0$. The statistics are all based on the minimized \overline{PWC} for each scheme with target value of N_t . The related simulation parameters are listed in Table 4 and the system's schematic is described in Section V-B, while the four-node network's topology is seen in Fig. 10 and the ten-node network's topology is seen in Fig. 19.

TABLE 11. The summary of the results extracted from Fig. 13 to Fig. 21. The statistics are all based on the minimized \overline{PWC} for each scheme given $N_t = 7$. The related simulation parameters are listed in Table 4 and the system's schematic is described in Section V-B, while the four-node network's topology is seen in Fig. 10 and the ten-node network's topology is seen in Fig. 19.

Code	TTCM	
Modulation	4QAM, HM-16QAM	
N_t	7	
Positions of the nodes	4-node system—Table VIII 10-node system—Table X	
\mathcal{P}_t of the nodes	4-node system—Table VIII 10-node system—Table X	
Constraints on Delay	95% plus of packets received	
Constraints on \mathcal{P}_t	\overline{PWC} of all schemes are minimized	
	Opt. \overline{PWC} mw	Φ [packet/TS]
HMOR 4-nodes system	0.7423	0.2200
HMOR 10-nodes system	0.2714	0.1324
	Outage P_{outage}	Delay (TS)
HMOR 4-nodes system L_1	0.0210	9 (97.33%)
HMOR 4-nodes system L_2	0.0239	15 (97.04%)
HMOR 10-nodes system L_1	0.0472	12 (96.92%)
HMOR 10-nodes system L_2	0.1836	19 (95.86%)

L_1 packets may be received by the ten-node network within a maximum of 12 TSs delay. By contrast, it may take 19 TSs for the DN to receive L_2 . In conclusion, the related simulation results are summarized in Table 11.

VIII. DESIGN GUIDELINES

Although we use TTCM as the channel code throughout this treatise, the HM based design can be generalized to any arbitrary coding schemes. In this section, we will summarize the general design guidelines of the coded HM based cooperative communication schemes investigated throughout [58]–[61], followed by the design guidelines of coded HM based OR algorithms conceived for *ad hoc* networks.

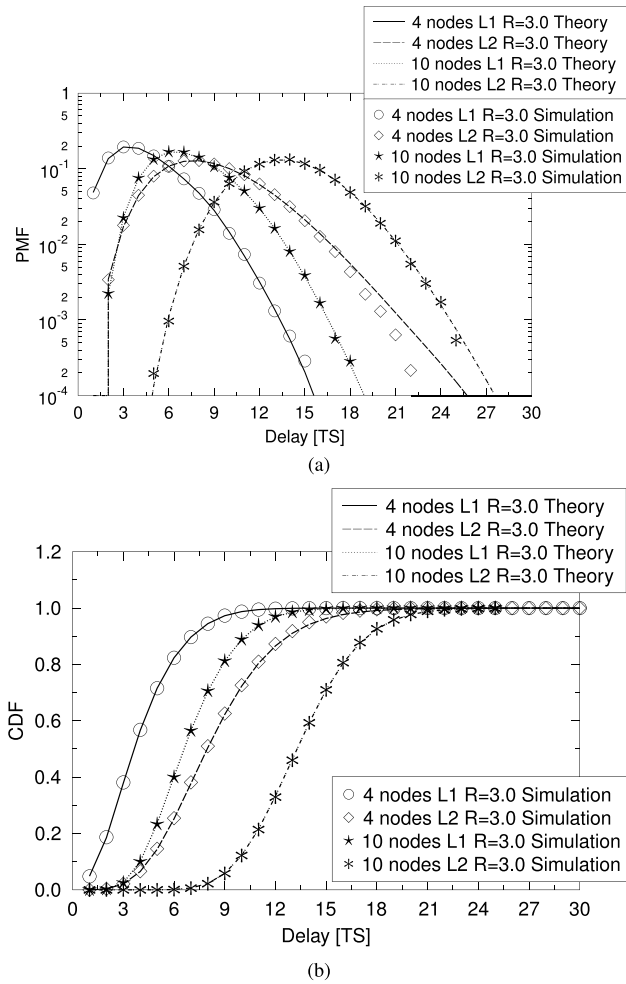


FIGURE 21. The PMF and the CDF of delay of the cooperative network based on our HMOR schemes with different number of hops. The packet transmitted is TCM aided HM-16QAM signals and the HM ratio is $R_1 = 3.0$. The statistics are all based on the minimized \overline{PWC} for each scheme given $N_t = 7$. The related simulation parameters are listed in Table 4 and the system's schematic is described in Section V-B, while the four-node network's topology is seen in Fig. 10 and the ten-node network's topology is seen in Fig. 19. (a) PMF of the delay for $N_t = 7$. (b) CDF of the delay for $N_t = 7$.

1) Coded HM Design for Cooperative Communications:

a) First, we have to identify, which specific HM features we want to exploit. In [60], our design objective is to exploit the UEP capability provided by the HM scheme in order to assist the transmission of a single coded information sequence in the context of cooperative communications. By contrast, in [58] and [59], our design goal is to assist the transmission of multiple independent information streams with the aid of coded HM schemes. The general idea is to exploit the specific features of the HM scheme to reduce the SNR_t of the SN and to invoke DAF based RNs for the sake of achieving a cooperative diversity gain.

b) Then, we appropriately design the RN(s) according to the overall system concept. In the HM based cooperative communication design, we always assume that the highest-priority layer of the multi-layer HM signals may be adequately received by the DN for the sake of maintaining the target-integrity requirement, provided that a sufficient high SNR_t can be achieved at the DN. In that case, the lower-priority layers may be forwarded to the DN by the DAF based RN(s). On the other hand, if the triple-layer HM-64QAM scheme of [58] is employed, the RN may have to forward two layers of its information to the DN. Nonetheless, in [58] and [59], each RN only has to forward a single layer of the information. More explicitly, the soft-information required for the target decoder should be specifically derived, as detailed in [58]–[60].

c) Finally, the optimization of the overall system depends on the choice of HM constellations, on the positions of the RNs, as well as on the required SNR_t of each nodes in the networks. In [58]–[60], the HM constellations may be appropriately modified by employing different HM ratios. Furthermore, the reduced path-loss facilitated by the employment of DAF based RNs may also influence the SNR_t required for adequately receiving the desired signals. Hence, to find the minimum \overline{SNR}_t for the entire system, multiple factors have to be taken into consideration.

2) Coded HM Design for Opportunistic Routing:

a) Firstly, we determine the specific choice of the cooperative strategies to be used by the wireless *ad hoc* networks, as discussed in Section V. In each transmission TS, only one of the nodes is activated for transmission. The transmission rules should be specially designed, as detailed in Section V-B. After determining the FER versus SNR curve, the performance of the system may be simulated using **Algorithm 2** of Section VI and the related system characteristics may be derived.

b) Then, we have to determine the legitimate system states and the transition probabilities in the system, as detailed in Section V-B and Section V-C. More specifically, according to the FER versus SNR function derived in Section V-A, the one-step state-transition probability matrix of the entire cooperative system may be computed, which is illustrated in Table 7. Similarly, the related characteristics of the HM based OR algorithm aided *ad hoc* network may be analysed theoretically by using **Algorithm 1**, as detailed in Section V-D.

c) Finally, we have to compare the simulation results to the theoretical analysis, as discussed

in Section VII. Then the minimum power consumption of the cooperative network may be derived, as determined by the position of the RNs, as well as by the specific transmit power of each node.

IX. FUTURE WORK

A. THEORETICAL ANALYSIS OF THE DCMC CAPACITY OF THE COOPERATION AIDED CODED HM SCHEME

In [58] and [59], the DCMC capacity was relied upon for analysing the achievable performance of the coded HM based cooperative scheme. However, the results were derived by simulations only, albeit it is desirable to arrive at a theoretical solution. Recall that the CCMC and DCMC capacities were first considered by Cover and Gamal in [138], where the general upper bound of the CCMC capacity of a half-duplex relay-aided system was derived in [139]. We have appropriately adapted the approach of [140] and [141] for deriving the DCMC capacity of our HM aided cooperative communication system. As mentioned in [58] and [59], the DCMC capacity is dependent on the specific choice of the modulation scheme, which is more pertinent for the design of practical channel-coded modulation schemes. However, the actual network capacity of even a single-relay based network is an open problem, whilst here we have multiple relays in our system, which are associated with multiple independent transmission links. The theoretical analysis of a complex system like this would be complex and would require various strong assumptions. Hence, an accurate and yet tractable less complex theoretical analysis would be very attractive.

B. NEAR-CAPACITY HM DESIGN FOR COOPERATIVE COMMUNICATION

The fundamental goal of the analysis presented in [58] and [59] is to quantify the modulation-dependent DCMC capacity of our system in order to analyse the achievable performance of the coded HM scheme. According to the specific cooperative strategy proposed in [58] and [59], we aim for finding the minimum energy-consumption based configuration of the system operating at the target rate, assuming that a ‘perfect’ capacity-achieving channel coding scheme is employed. These results may be considered as the lower bound conceived for guiding the design of HM schemes employing a realistic channel encoder within the same cooperative framework. In [58], we have employed both TTCM and LDPC codes in another HM based cooperative communication scheme. However, a range of other powerful near-capacity source/channel codes, including turbo codes, Variable Length Code (VLC) [142], polar codes [143] etc may be employed. The constellations of the HM and of the source/channel encoder may be designed jointly for approaching the achievable capacity.

C. ADAPTIVE HM AIDED COOPERATIVE COMMUNICATIONS

One of the most significant merits of the HM scheme is its high flexibility, which is particularly beneficial in conjunction with adaptive modulation schemes. The adaptive HM theory was provided by Hossain in [7] and [8], where the multiple independent information streams may also be combined by the HM scheme. However, the activated constellation of the transmitted HM-based source signal directly depends on the channel quality. To be more specific, assuming that three independent signal streams are broadcast by the SN, when the channel conditions are good, the SN may activate the triple-layer HM scheme for transmitting all three layers of information simultaneously. However, when the channel conditions are poorer, the SN may activate a twin-layer HM scheme for transmitting the most important two layers of information or even using conventional BPSK/4QAM modulation scheme for transmitting a single layer consisting of the highest-priority information. Hence, the adaptive HM may be deemed to be a convenient application-oriented modulation scheme. Explicitly, the fundamental goal is to guarantee that during each transmission session, the information contained in the transmitted signal may be successfully received by the DN. By incorporating the adaptive HM scheme, both the flexibility and the reliability of the cooperative system may be further improved in order to approach its DCMC capacity more closely.

D. SPATIAL MODULATION AIDED HM IN COOPERATIVE COMMUNICATION

Spatial Modulation (SM) may be the most direct and compelling method of improving the performance of the HM based cooperative communication system. In [144], Mesleh *et al.* discussed the performance of the SM scheme in detail, where the information is embedded both into the classic transmitted symbol streams and into the unique transmit antenna indices chosen from a set of transmit antennas according to the information to be transmitted. Note that activating one out of N_t transmit antennas may allow us to convey $\log_2 N_t$ extra bits. Hence, for the same throughput, the SM aided transmitter may employ a lower-order modulation scheme for the activated antenna. This would require a lower SNR_t^{SN} for achieving the same BER, whilst additionally requiring fewer RF chains than the conventional MIMO modulation schemes. Additionally, in contrast to the classic MIMO schemes, such as the Diagonal Bell Laboratories Layered Space-Time (D-BLAST) or the Vertical BLAST (V-BLAST), the Inter Channel Interference (ICI) may be avoided, because only a single transmit antenna of the entire set will be activated by the SM scheme. Furthermore, the need for synchronizing several transmit antennas may also be avoided. Hence, some of the disadvantages of the classic MIMO schemes may be circumvented.

E. HIGH-ORDER HM AIDED COOPERATIVE COMMUNICATION IN AD HOC NETWORKS

We have introduced the twin-layer coded HM concept for transmission over wireless *ad hoc* networks in this paper. More specifically, the OR algorithm based cooperative system was beneficially assisted by the HM scheme. Both the theoretical analysis as well as the simulation-based study of the resultant cooperative system were presented in detail in Section V and Section VI. It may be observed that when assuming that the packets transmitted over the networks are layered-modulation signals, the power-efficiency of the entire cooperative network is improved by partitioning the HM-based multiple layer packets into sub-packets during this transmission. However, the HM scheme proposed in this paper is the simplest twin-layer HM-16QAM scheme. When higher-order HM schemes are considered, the resultant cooperative strategy may become more flexible. On the other hand, when considering a triple-layer HM-64QAM scheme in the context of a four-node cooperative network, the complexity of the cooperative network is increased dramatically. Explicitly, the number of the legitimate states of a triple-layer HM-64QAM aided four-node network may be computed as:

$$N_{state} = \frac{1 \times 2}{2} + \frac{2 \times 3}{2} + \frac{3 \times 4}{2} + \frac{4 \times 5}{2} = 20. \quad (35)$$

Furthermore, the number of the possible states of a triple-layer HM-64QAM aided n -node network may be calculated as:

$$\begin{aligned} N_{state} &= \frac{1 \times 2}{2} + \frac{2 \times 3}{2} + \dots + \frac{n \times (n+1)}{2} \\ &= \sum_{i=1}^n \frac{i \times (i+1)}{2}. \end{aligned} \quad (36)$$

Hence, the increased number of states N_{state} and the potential destination target of the nodes in the network results in a complex one-step state-transition probability matrix. Additionally, we should also take into account the position of the nodes, the transmission power of the nodes in the network as well as the specific relay selection algorithms, when analysing the characteristics of the cooperative Network.

F. CODED HM BASED BUFFER-AIDED MULTIHOP COOPERATIVE COMMUNICATION

Recently, buffer-aided cooperative communications over wireless *ad hoc* networks has drawn a lot of research interests [145]–[147]. More explicitly, the RNs are capable of temporarily storing a fixed or a flexible number of packets using buffers. When the channel conditions are poor, the RN may still be able to receive information from the SN and only forward it to DN, when the quality of the RN-DN link has been sufficiently improved. In [124], the authors investigated the performance of a buffer-aided OR algorithm in the context of *ad hoc* networks. They proved that both the throughput and the power-efficiency of the buffer-aided OR algorithm based cooperative networks are better than that of the traditional OR algorithm based cooperative networks.

Note that the conventional OR algorithm aims for searching for the optimum SN-RN, RN-RN, RN-DN links step by step, while the buffer-aided RN is more flexible in terms of deciding, when to transmit and when to receive according to the corresponding channel conditions. Hence, the combination of these two algorithms may be capable of improving the probability of successful transmission across each link. Therefore, both the outage probability and the average packet power consumption may be reduced. However, the buffer-aided OR algorithm is not suitable for delay sensitive systems. The benefits that conventional relaying may offer for delay-sensitive systems is that the conventional relaying avoids the buffering delay [145]. By employing our HM scheme, the higher delay of the buffer-aided OR algorithm may be mitigated, because the delay-sensitive information may be mapped to the higher-protected layer of the HM symbols for the sake of achieving a lower delay, while the delay-tolerant information may be mapped to contained in the lower-protected layer and be forwarded to the DN following the routes decided by the buffer-aided OR algorithm. Therefore, the delay-sensitive and the delay-tolerant information may be transmitted simultaneously, while a high average throughput may be achieved with the aid of an appropriately designed HM scheme.

X. CONCLUSIONS

In this paper, we mainly focus our attention on the cooperative network transmitting layered packets. We firstly characterized the FER versus SNR performance of receiving both L_1 and L_2 of the TTCM coded twin-layer HM-16QAM signals, as well as that of receiving TTCM coded 4QAM signals for transmission over both AWGN and Rayleigh-distributed block fading channels. Secondly, the cooperative communication protocol of our HMOR scheme of Section V has been illustrated. Furthermore, we detailed our theoretical analysis and our simulation method conceived for characterizing the HMOR scheme. The simulation results have demonstrated that our theoretical analysis is confirmed by our simulations. We have also demonstrated that our HMOR scheme is more flexible and more power-efficient than its TOR benchmark. By partitioning the layered modulated packets according to their specific reception rule, the power \mathcal{P}_T of each single node in the network, as well as the average per-packet power consumption \overline{PWC} of the entire system may be reduced. There is a trade-off between the power-efficiency and delay. Explicitly, our HMOR scheme may require longer time to receive the entire twin-layer packet, whilst the outage probability of the more important information layer L_1 of the twin-layer HM-16QAM packets is reduced. In our future work, buffer-aided cooperative communication will be taken into consideration [145], [146]. Explicitly, the RN may be capable of temporarily storing a number of packets using buffers, where the forwarding process will depend on the instantaneous channel condition. Consequently, the probability of successful transmission among the nodes may be increased and the throughput of the cooperative network may also be improved. Additionally, the HM with three or more layers

may also be considered for increasing the data rate of the entire cooperative network.

REFERENCES

- [1] M. El-Hajjar and L. Hanzo, "A survey of digital television broadcast transmission techniques," *IEEE Commun. Surveys Tuts.*, vol. 15, no. 4, pp. 1924–1949, Apr. 2013.
- [2] B. Baumgartner. (May 2005). *Europe: HD Ready?* [Online]. Available: <http://www.eetimes.com>
- [3] C. Hellge, S. Mirta, T. Schierl, and T. Wiegand, "Mobile TV with SVC and hierarchical modulation for DVB-H broadcast services," in *Proc. IEEE Int. Symp. Broadband Multimedia Syst. Broadcast. (BMSB)*, May 2009, pp. 1–5.
- [4] S. Wang, S. Kwon, and B. K. Yi, "On enhancing hierarchical modulation," in *Proc. IEEE Int. Symp. Broadband Multimedia Syst. Broadcast.*, Mar./Apr. 2008, pp. 1–6.
- [5] R. Y. Kim and Y. Y. Kim, "Symbol-level random network coded cooperation with hierarchical modulation in relay communication," *IEEE Trans. Consum. Electron.*, vol. 55, no. 3, pp. 1280–1285, Aug. 2009.
- [6] H. Jiang and P. A. Wilford, "A hierarchical modulation for upgrading digital broadcast systems," *IEEE Trans. Broadcast.*, vol. 51, no. 2, pp. 223–229, Jun. 2005.
- [7] M. J. Hossain, P. K. Vitthaladevuni, M.-S. Alouini, and V. K. Bhargava, "Adaptive hierarchical modulation for simultaneous voice and multiclass data transmission over fading channels," *IEEE Trans. Veh. Technol.*, vol. 55, no. 4, pp. 1181–1194, Jul. 2006.
- [8] M. J. Hossain, M.-S. Alouini, and V. K. Bhargava, "Rate adaptive hierarchical modulation-assisted two-user opportunistic scheduling," *IEEE Trans. Wireless Commun.*, vol. 6, no. 6, pp. 2076–2085, Jun. 2007.
- [9] M.-K. Chang and S.-Y. Lee, "Performance analysis of cooperative communication system with hierarchical modulation over Rayleigh fading channel," *IEEE Trans. Wireless Commun.*, vol. 8, no. 6, pp. 2848–2852, Jun. 2009.
- [10] S. Y. Lee and K. C. Whang, "A collaborative cooperation scheme using hierarchical modulation," in *Proc. IEEE 68th Veh. Technol. Conf. (VTC)*, Sep. 2008, pp. 1–5.
- [11] S.-H. Chang, M. Rim, P. C. Cosman, and L. B. Milstein, "Optimized unequal error protection using multiplexed hierarchical modulation," *IEEE Trans. Inf. Theory*, vol. 58, no. 9, pp. 5816–5840, Sep. 2012.
- [12] Y. Noli, H. Lee, W. Lee, and L. Lee, "Design of unequal error protection for MIMO-OFDM systems with hierarchical signal constellations," *J. Commun. Netw.*, vol. 9, no. 2, pp. 167–176, Jun. 2007.
- [13] Y. C. Chang, S. W. Lee, and R. Komiya, "A low complexity hierarchical QAM symbol bits allocation algorithm for unequal error protection of wireless video transmission," *IEEE Trans. Consum. Electron.*, vol. 55, no. 3, pp. 1089–1097, Aug. 2009.
- [14] K. M. Alajel, W. Xiang, and Y. Wang, "Unequal error protection scheme based hierarchical 16-QAM for 3-D video transmission," *IEEE Trans. Consum. Electron.*, vol. 58, no. 3, pp. 731–738, Aug. 2012.
- [15] S. S. Arslan, P. C. Cosman, and L. B. Milstein, "Coded hierarchical modulation for wireless progressive image transmission," *IEEE Trans. Veh. Technol.*, vol. 60, no. 9, pp. 4299–4313, Nov. 2011.
- [16] S. S. Arslan, P. C. Cosman, and L. B. Milstein, "On hard decision upper bounds for coded M -ary hierarchical modulation," in *Proc. 45th Annu. Conf. Inf. Sci. Syst. (CISS)*, Mar. 2011, pp. 1–6.
- [17] C. Hausl and J. Hagenauer, "Relay communication with hierarchical modulation," *IEEE Commun. Lett.*, vol. 11, no. 1, pp. 64–66, Jan. 2007.
- [18] L. L. Hanzo, T. H. Liew, B. L. Yeap, R. Y. S. Tee, and S. X. Ng, *Turbo Coding, Turbo Equalisation and Space-Time Coding: EXIT-Chart-Aided Near-Capacity Designs for Wireless Channels*, 2nd ed. New York, NY, USA: Wiley, 2011.
- [19] C.-H. Choi, Y.-J. Kim, and G.-H. Im, "Bit-interleaved coded transmission with multilevel modulation for non-orthogonal cooperative systems," *IEEE Trans. Commun.*, vol. 59, no. 1, pp. 95–105, Jan. 2011.
- [20] Z. Li, M. Peng, and W. Wang, "Hierarchical modulated channel and network coding scheme in the multiple-access relay system," in *Proc. IEEE 13th Int. Conf. Commun. Technol. (ICCT)*, Sep. 2011, pp. 984–988.
- [21] J. M. Park, S.-L. Kim, and J. Choi, "Hierarchically modulated network coding for asymmetric two-way relay systems," *IEEE Trans. Veh. Technol.*, vol. 59, no. 5, pp. 2179–2184, Jun. 2010.
- [22] Z. Du, P. Hong, K. Xue, and J. Peng, "Hierarchically modulated coded cooperation for relay system," in *Proc. IEEE Consum. Commun. Netw. Conf. (CCNC)*, Jan. 2012, pp. 812–816.
- [23] D.-K. Kwon, W.-J. Kim, K.-H. Suh, H. Lim, and H.-N. Kim, "A higher data-rate T-DMB system based on a hierarchical A-DPSK modulation," *IEEE Trans. Broadcast.*, vol. 55, no. 1, pp. 42–50, Mar. 2009.
- [24] P. Robertson and T. Würz, "Bandwidth-efficient turbo trellis-coded modulation using punctured component codes," *IEEE J. Sel. Areas Commun.*, vol. 16, no. 2, pp. 206–218, Feb. 1998.
- [25] S. X. Ng, J. Y. Chung, and L. Hanzo, "Turbo-detected unequal protection MPEG-4 wireless video telephony using multi-level coding, trellis coded modulation and space-time trellis coding," *IEE Proc.-Commun.*, vol. 152, no. 6, pp. 1116–1124, Dec. 2005.
- [26] S. X. Ng, C. Qian, D. Liang, and L. Hanzo, "Adaptive turbo trellis coded modulation aided distributed space-time trellis coding for cooperative communications," in *Proc. IEEE 71st Veh. Technol. Conf. (VTC-Spring)*, May 2010, pp. 1–5.
- [27] S. X. Ng, J. Wang, and L. Hanzo, "Unveiling near-capacity code design: The realization of Shannon's communication theory for MIMO channels," in *Proc. IEEE Int. Conf. Commun. (ICC)*, May 2008, pp. 1415–1419.
- [28] S. X. Ng, T. H. Liew, L.-L. Yang, and L. Hanzo, "Comparative study of TCM, TTCM, BICM and BICM-ID schemes," in *Proc. IEEE VTS 53rd Veh. Technol. Conf.*, Rhodes, Greece, May 2010, pp. 2450–2454.
- [29] S. X. Ng, K. Zhu, and L. Hanzo, "Distributed source-coding, channel-coding and modulation for cooperative communications," in *Proc. IEEE 72nd Veh. Technol. Conf. Fall (VTC-Fall)*, Sep. 2010, pp. 1–5.
- [30] S. X. Ng, O. R. Alamri, Y. Li, J. Kliewer, and L. Hanzo, "Near-capacity turbo trellis coded modulation design based on EXIT charts and union bounds," *IEEE Trans. Commun.*, vol. 56, no. 12, pp. 2030–2039, Dec. 2008.
- [31] R. W. Lucky and J. C. Hancock, "On the optimum performance of N -ary systems having two degrees of freedom," *IRE Trans. Commun. Syst.*, vol. 10, no. 2, pp. 185–192, Jun. 1962.
- [32] T. M. Cover, "Broadcast channels," *IEEE Trans. Inf. Theory*, vol. 18, no. 1, pp. 2–14, Jan. 1972.
- [33] P. Bergmans and T. M. Cover, "Cooperative broadcasting," *IEEE Trans. Inf. Theory*, vol. 20, no. 3, pp. 317–324, May 1974.
- [34] K. Fazel and M. Ruf, "Combined multilevel coding and multiresolution modulation," in *Proc. Tech. Program, Conf. Rec., IEEE Int. Conf. Commun. (ICC)*, vol. 2. Geneva, Switzerland, May 1993, pp. 1081–1085.
- [35] L. Hanzo, S. X. Ng, T. Keller, and W. Webb, *Quadrature Amplitude Modulation From Basics to Adaptive Trellis-Coded, Turbo-Equalised and Space-Time Coded OFDM, CDMA and MC-CDMA Systems*, 2nd ed. New York, NY, USA: Wiley, 2004.
- [36] M. Morimoto, M. Okada, and S. Komaki, "Joint on-board resource sharing and hierarchical modulation scheme for satellite communication," in *Proc. IEEE Global Telecommun. Conf.*, vol. 3. Nov. 1995, pp. 1662–1666.
- [37] M. Morimoto, M. Okada, and S. Komaki, "A hierarchical image transmission system for multimedia mobile communication," in *Proc. 1st Int. Workshop Wireless Image/Video Commun.*, Sep. 1996, pp. 80–84.
- [38] S. O'Leary, "Hierarchical transmission and COFDM systems," *IEEE Trans. Broadcast.*, vol. 43, no. 2, pp. 166–174, Jun. 1997.
- [39] V. Engels and H. Rohling, "Multi-resolution 64-DAPSK modulation in a hierarchical COFDM transmission system," *IEEE Trans. Broadcast.*, vol. 44, no. 1, pp. 139–149, Mar. 1998.
- [40] D. W. Schill, D.-F. Yuan, and J. B. Huber, "Efficient hierarchical broadcasting using multilevel codes," in *Proc. Inf. Theory Netw. Workshop*, Jun./Jul. 1999, p. 72.
- [41] C. Nokes and J. Mitchell, "Potential benefits of hierarchical modes of the DVB-T specification," in *Proc. IEE Colloq. Digit. Television*, 1999, pp. 10/1–10/6.
- [42] A. Seegert, "Broadcast communication on fading channels using hierarchical coded modulation," in *Proc. IEEE Global Telecommun. Conf.*, vol. 1. Nov. 2000, pp. 92–97.
- [43] P. K. Vitthaladevuni and M.-S. Alouini, "BER computation of $4/M$ -QAM hierarchical constellations," *IEEE Trans. Broadcast.*, vol. 47, no. 3, pp. 228–239, Sep. 2001.
- [44] C.-S. Hwang and Y. Kim, "An adaptive modulation method for multicast communications of hierarchical data in wireless networks," in *Proc. IEEE Int. Conf. Commun.*, vol. 2. Apr./May 2002, pp. 869–900.
- [45] P. K. Vitthaladevuni and M.-S. Alouini, "A recursive algorithm for the exact BER computation of generalized hierarchical QAM constellations," *IEEE Trans. Inf. Theory*, vol. 49, no. 1, pp. 297–307, Jan. 2003.

- [46] J. Pons, P. Duvaud, O. Moreno, and L. Pierrugues, "Enhanced TCM based on a multilevel hierarchical trellis coded modulation (HTCM)," in *Proc. IEEE Global Telecommun. Conf.*, vol. 4, Nov./Dec. 2004, pp. 2589–2593.
- [47] B. Barmada, M. M. Ghandi, E. V. Jones, and M. Ghanbari, "Prioritized transmission of data partitioned H.264 video with hierarchical QAM," *IEEE Signal Process. Lett.*, vol. 12, no. 8, pp. 577–580, Aug. 2005.
- [48] M. J. Hossain, P. K. Vitthaladevuni, M.-S. Alouini, and V. K. Bhargava, "Hierarchical modulations for multimedia and multicast transmission over fading channels," in *Proc. 57th IEEE Semiannu. Veh. Technol. Conf. (VTC-Spring)*, vol. 4, Apr. 2003, pp. 2633–2637.
- [49] M. J. Hossain, M.-S. Alouini, and V. K. Bhargava, "Hierarchical constellation for multi-resolution data transmission over block fading channels," *IEEE Trans. Wireless Commun.*, vol. 5, no. 4, pp. 849–857, Apr. 2006.
- [50] Y. C. Chang, S. W. Lee, and R. Komiya, "A low-complexity unequal error protection of H.264/AVC video using adaptive hierarchical QAM," *IEEE Trans. Consum. Electron.*, vol. 52, no. 4, pp. 1153–1158, Nov. 2006.
- [51] S. Wang and B. K. Yi, "Optimizing enhanced hierarchical modulations," in *Proc. IEEE Global Telecommun. Conf.*, Nov./Dec. 2008, pp. 1–5.
- [52] M. Peng, Y. Liu, D. Wei, W. Wang, and H.-H. Chen, "Hierarchical cooperative relay based heterogeneous networks," *IEEE Wireless Commun.*, vol. 18, no. 3, pp. 48–56, Jun. 2011.
- [53] Z. Hu and H. Liu, "A low-complexity LDPC decoding algorithm for hierarchical broadcasting: Design and implementation," *IEEE Trans. Veh. Technol.*, vol. 62, no. 4, pp. 1843–1849, May 2012.
- [54] X. Wang and L. Cai, "Proportional fair scheduling in hierarchical modulation aided wireless networks," *IEEE Trans. Wireless Commun.*, vol. 12, no. 4, pp. 1584–1593, Apr. 2013.
- [55] H. Meric, J. Lacan, F. Arnal, G. Lesthievant, and M.-L. Boucheret, "Combining adaptive coding and modulation with hierarchical modulation in Satcom systems," *IEEE Trans. Broadcast.*, vol. 59, no. 4, pp. 627–637, Dec. 2013.
- [56] B. Mouhouche, A. Mourad, and D. Ansoregui, "Throughput optimization of precoded OFDM with hierarchical modulation," in *Proc. 7th Int. Conf. Signal Process. Commun. Syst. (ICSPCS)*, Dec. 2013, pp. 1–10.
- [57] A. Saeed, H. Xu, and T. Quazi, "Alamouti space-time block coded hierarchical modulation with signal space diversity and MRC reception in Nakagami- m fading channel," *IET Commun.*, vol. 8, no. 4, pp. 516–524, Mar. 2014.
- [58] H. Sun, S. X. Ng, C. Dong, and L. Hanzo, "Decode-and-forward cooperation-aided triple-layer turbo-trellis-coded hierarchical modulation," *IEEE Trans. Commun.*, vol. 63, no. 4, pp. 1136–1148, Apr. 2015.
- [59] H. Sun, S. X. Ng, and L. Hanzo, "Turbo trellis-coded hierarchical-modulation assisted decode-and-forward cooperation," *IEEE Trans. Veh. Technol.*, vol. 64, no. 9, pp. 3971–3981, Sep. 2014.
- [60] H. Sun, Y. Shen, S. X. Ng, and L. Hanzo, "Turbo trellis coded hierarchical modulation for cooperative communications," in *Proc. IEEE Wireless Commun. Netw. Conf. (WCNC)*, Apr. 2013, pp. 2789–2794.
- [61] H. Sun, S. X. Ng, and L. Hanzo, "Superposition coded modulation for cooperative communications," in *Proc. IEEE Veh. Technol. Conf. (VTC Fall)*, Sep. 2012, pp. 1–5.
- [62] H. Labiod, Ed., *Wireless Ad Hoc and Sensor Networks*. New York, NY, USA: Wiley, 2010.
- [63] S.-L. Wu and Y.-C. Tseng, Eds., *Wireless Ad Hoc Networking: Personal-Area, Local-Area, and the Sensory-Area Networks*. New York, NY, USA: Auerbach, 2007.
- [64] D. B. Johnson, "Routing in ad hoc networks of mobile hosts," in *Proc. Workshop Mobile Comput. Syst. Appl.*, Dec. 1994, pp. 158–163.
- [65] R. L. Davies, R. M. Watson, A. Munro, and M. H. Barton, "Ad-hoc wireless networking: Contention free multiple access," in *Proc. 5th IEEE Conf. Telecommun.*, Mar. 1995, pp. 73–77.
- [66] B. Das and V. Bhargavan, "Routing in ad-hoc networks using minimum connected dominating sets," in *Proc. IEEE Int. Conf. Commun. (ICC)*, vol. 1, Montreal, QC, Canada, Jun. 1997, pp. 376–380.
- [67] J. Broch, D. A. Maltz, and D. B. Johnson, "Supporting hierarchy and heterogeneous interfaces in multi-hop wireless ad hoc networks," in *Proc. 4th Int. Symp. Parallel Archit., Algorithms, Netw.*, Jun. 1999, pp. 370–375.
- [68] U. Jonsson, F. Alriksson, T. Larsson, P. Johansson, and G. Q. Maguire, Jr., "MIPMANET-mobile IP for mobile ad hoc networks," in *Proc. 1st Annu. Workshop Mobile Ad Hoc Netw. Comput.*, 2000, pp. 75–85.
- [69] D. Niculescu and B. Nath, "Ad hoc positioning system (APS)," in *Proc. IEEE Global Telecommun. Conf.*, vol. 5, Nov. 2001, pp. 2926–2931.
- [70] M. Grossglauser and D. N. C. Tse, "Mobility increases the capacity of ad hoc wireless networks," *IEEE/ACM Trans. Netw.*, vol. 10, no. 4, pp. 477–486, Aug. 2002.
- [71] M. Zorzi and R. R. Rao, "Geographic random forwarding (GeRaF) for ad hoc and sensor networks: Multihop performance," *IEEE Trans. Mobile Comput.*, vol. 2, no. 4, pp. 337–348, Oct./Dec. 2003.
- [72] O. Younis and S. Fahmy, "HEED: A hybrid, energy-efficient, distributed clustering approach for ad hoc sensor networks," *IEEE Trans. Mobile Comput.*, vol. 3, no. 4, pp. 366–379, Oct./Dec. 2004.
- [73] S. P. Weber, X. Yang, J. G. Andrews, and G. de Veciana, "Transmission capacity of wireless ad hoc networks with outage constraints," *IEEE Trans. Inf. Theory*, vol. 51, no. 12, pp. 4091–4102, Dec. 2005.
- [74] L. Pelusi, A. Passarella, and M. Conti, "Opportunistic networking: Data forwarding in disconnected mobile ad hoc networks," *IEEE Commun. Mag.*, vol. 44, no. 11, pp. 134–141, Nov. 2006.
- [75] J. Zhao and G. Cao, "VADD: Vehicle-assisted data delivery in vehicular ad hoc networks," *IEEE Trans. Veh. Technol.*, vol. 57, no. 3, pp. 1910–1922, May 2008.
- [76] J. Harri, F. Filali, and C. Bonnet, "Mobility models for vehicular ad hoc networks: A survey and taxonomy," *IEEE Commun. Surveys Tuts.*, vol. 11, no. 4, pp. 19–41, Dec. 2009.
- [77] O. K. Tonguz, N. Wisitpongphan, and F. Bai, "DV-CAST: A distributed vehicular broadcast protocol for vehicular ad hoc networks," *IEEE Wireless Commun.*, vol. 17, no. 2, pp. 47–57, Apr. 2010.
- [78] S.-J. Kim and G. B. Giannakis, "Optimal resource allocation for MIMO ad hoc cognitive radio networks," *IEEE Trans. Inf. Theory*, vol. 57, no. 5, pp. 3117–3131, May 2011.
- [79] A. A. Bhorkar, M. Naghshvar, T. Javidi, and B. D. Rao, "Adaptive opportunistic routing for wireless ad hoc networks," *IEEE/ACM Trans. Netw.*, vol. 20, no. 1, pp. 243–256, Feb. 2011.
- [80] K. Huang, "Spatial throughput of mobile ad hoc networks powered by energy harvesting," *IEEE Trans. Inf. Theory*, vol. 59, no. 11, pp. 7597–7612, Nov. 2013.
- [81] J. Zuo, C. Dong, H. V. Nguyen, S. X. Ng, L.-L. Yang, and L. Hanzo, "Cross-layer aided energy-efficient opportunistic routing in ad hoc networks," *IEEE Trans. Commun.*, vol. 62, no. 2, pp. 522–535, Feb. 2014.
- [82] V. Sharma and R. Kumar, "An opportunistic cross layer design for efficient service dissemination over flying ad hoc networks (FANETs)," in *Proc. 2nd Int. Conf. Electron. Commun. Syst. (ICECS)*, Feb. 2015, pp. 1551–1557.
- [83] M. Mauve, J. Widmer, and H. Hartenstein, "A survey on position-based routing in mobile ad hoc networks," *IEEE Netw.*, vol. 15, no. 6, pp. 30–39, Nov./Dec. 2001.
- [84] H. Liu, B. Zhang, H. T. Mouftah, X. Shen, and J. Ma, "Opportunistic routing for wireless ad hoc and sensor networks: Present and future directions," *IEEE Commun. Mag.*, vol. 47, no. 12, pp. 103–109, Dec. 2009.
- [85] K. Zeng, W. Lou, and H. Zhai, "Capacity of opportunistic routing in multi-rate and multi-hop wireless networks," *IEEE Trans. Wireless Commun.*, vol. 7, no. 12, pp. 5118–5128, Dec. 2008.
- [86] S. Biswas and R. Morris, "ExOR: Opportunistic multi-hop routing for wireless networks," in *Proc. ACM SIGCOMM*, 2005, pp. 133–144.
- [87] S. Chachulski, M. Jennings, S. Katti, and D. Katabi, "Trading structure for randomness in wireless opportunistic routing," in *Proc. ACM SIGCOMM*, 2007, pp. 169–180.
- [88] Y. Li, A. Mohaisen, and Z.-L. Zhang, "Trading optimality for scalability in large-scale opportunistic routing," *IEEE Trans. Veh. Technol.*, vol. 62, no. 5, pp. 2253–2263, Jun. 2012.
- [89] R. Leung, J. Liu, E. Poon, A.-L. C. Chan, and B. Li, "MP-DSR: A QoS-aware multi-path dynamic source routing protocol for wireless ad-hoc networks," in *Proc. 26th Annu. IEEE Conf. Local Comput. Netw. (LCN)*, Nov. 2001, pp. 132–141.
- [90] C. E. Perkins and E. M. Royer, "Ad-hoc on-demand distance vector routing," in *Proc. 2nd IEEE Workshop Mobile Comput. Syst. Appl. (WMCSA)*, Feb. 1999, pp. 90–100.
- [91] C. Lott and D. Teneketzis, "Stochastic routing in ad-hoc networks," *IEEE Trans. Autom. Control*, vol. 51, no. 1, pp. 52–70, Jan. 2006.
- [92] N. Chakchouk, "A survey on opportunistic routing in wireless communication networks," *IEEE Commun. Surveys Tuts.*, vol. 17, no. 4, pp. 2214–2241, Mar. 2015.
- [93] G. Y. Lee and Z. J. Haas, "Simple, practical, and effective opportunistic routing for short-haul multi-hop wireless networks," *IEEE Trans. Wireless Commun.*, vol. 10, no. 11, pp. 3583–3588, Nov. 2011.
- [94] X. Jin, R. Zhang, J. Sun, and Y. Zhang, "TIGHT: A geographic routing protocol for cognitive radio mobile ad hoc networks," *IEEE Trans. Wireless Commun.*, vol. 13, no. 8, pp. 4670–4681, Aug. 2014.

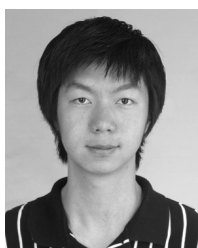
- [95] H. Füßler, J. Widmer, M. Käsemann, M. Mauve, and H. Hartenstein, "Contention-based forwarding for mobile ad hoc networks," *Ad Hoc Netw.*, vol. 1, no. 4, pp. 351–369, Nov. 2003.
- [96] B. Zhao, R. Seshadri, and M. C. Valenti, "Geographic random forwarding with hybrid-ARQ for ad hoc networks with rapid sleep cycles," in *Proc. IEEE Global Telecommun. Conf.*, vol. 5, Nov./Dec. 2004, pp. 3047–3052.
- [97] S. Biswas and R. Morris, "Opportunistic routing in multi-hop wireless networks," *ACM SIGCOMM Comput. Commun. Rev.*, vol. 34, no. 1, pp. 69–74, Jan. 2004.
- [98] Y. Yuan, H. Yang, S. H. Y. Wong, S. Lu, and W. Arbaugh, "ROMER: Resilient opportunistic mesh routing for wireless mesh networks," in *Proc. IEEE Workshop Wireless Mesh Netw. (WiMesh)*, Sep. 2005, pp. 1–9.
- [99] J. LeBrun, C.-N. Chuah, D. Ghosal, and M. Zhang, "Knowledge-based opportunistic forwarding in vehicular wireless ad hoc networks," in *Proc. IEEE 61st Veh. Technol. Conf. (VTC-Spring)*, vol. 4, May/June 2005, pp. 2289–2293.
- [100] C. Westphal, "Opportunistic routing in dynamic ad hoc networks: The OPRAH protocol," in *Proc. IEEE Int. Conf. Mobile Adhoc Sensor Syst.*, Oct. 2006, pp. 570–573.
- [101] E. Rozner, J. Seshadri, Y. Mehta, and L. Qiu, "Simple opportunistic routing protocol for wireless mesh networks," in *Proc. 2nd IEEE Workshop Wireless Mesh Netw.*, Sep. 2006, pp. 48–54.
- [102] Z. Zhong, J. Wang, G.-H. Lu, and S. Nelakuditi, "On selection of candidates for opportunistic anypath forwarding," in *Proc. Conf. ACM Special Interest Group Data Commun. (SIGCOMM)*, 2006, pp. 1–2.
- [103] K. Zeng, W. Lou, J. Yang, and D. R. Brown, III, "On throughput efficiency of geographic opportunistic routing in multihop wireless networks," *Mobile Netw. Appl.*, vol. 12, no. 5, pp. 347–357, Dec. 2007.
- [104] M. S. Nassr, J. Jun, S. J. Eidenbenz, A. A. Hansson, and A. M. Mielke, "Scalable and reliable sensor network routing: Performance study from field deployment," in *Proc. 26th IEEE Int. Conf. Comput. Commun. (INFOCOM)*, May 2007, pp. 670–678.
- [105] Y. Lin, B. Li, and B. Liang, "CodeOR: Opportunistic routing in wireless mesh networks with segmented network coding," in *Proc. IEEE Int. Conf. Netw. Protocols*, Oct. 2008, pp. 13–22.
- [106] D. Koutsonikolas, Y. C. Hu, and C.-C. Wang, "XCOR: Synergistic interflow network coding and opportunistic routing," in *Proc. ACM Annu. Int. Conf. Mobile Comput. Netw. (MobiCom)*, Sep. 2008, pp. 1–3.
- [107] V. Conan, J. Leguay, and T. Friedman, "Fixed point opportunistic routing in delay tolerant networks," *IEEE J. Sel. Areas Commun.*, vol. 26, no. 5, pp. 773–782, Jun. 2008.
- [108] K. Zeng, Z. Yang, and W. Lou, "Location-aided opportunistic forwarding in multirate and multihop wireless networks," *IEEE Trans. Veh. Technol.*, vol. 58, no. 6, pp. 3032–3040, Jul. 2008.
- [109] S. Yang, F. Zhong, C. K. Yeo, B. S. Lee, and J. Boleng, "Position based opportunistic routing for robust data delivery in MANETs," in *Proc. IEEE Global Telecommun. Conf.*, Nov./Dec. 2009, pp. 1–6.
- [110] R. Lauffer, H. Dubois-Ferriere, and L. Kleinrock, "Multirate anypath routing in wireless mesh networks," in *Proc. IEEE INFOCOM*, Apr. 2009, pp. 37–45.
- [111] Y. Lin, B. Liang, and B. Li, "SlideOR: Online opportunistic network coding in wireless mesh networks," in *Proc. IEEE INFOCOM*, Mar. 2010, pp. 1–5.
- [112] M. Naghshvar and T. Javidi, "Opportunistic routing with congestion diversity in wireless multi-hop networks," in *Proc. IEEE INFOCOM*, Mar. 2010, pp. 1–5.
- [113] A. Bletsas, A. G. Dimitriou, and J. N. Sahalos, "Interference-limited opportunistic relaying with reactive sensing," *IEEE Trans. Wireless Commun.*, vol. 9, no. 1, pp. 14–20, Jan. 2010.
- [114] X. Mao, S. Tang, X. Xu, X.-Y. Li, and H. Ma, "Energy-efficient opportunistic routing in wireless sensor networks," *IEEE Trans. Parallel Distrib. Syst.*, vol. 22, no. 11, pp. 1934–1942, Nov. 2011.
- [115] C. Y. Lee and G. U. Hwang, "Minimum energy consumption design of a two-hop relay network for QoS guarantee," in *Proc. Wireless Telecommun. Symp. (WTS)*, Apr. 2010, pp. 1–6.
- [116] X. Fang, D. Yang, and G. Xue, "Consort: Node-constrained opportunistic routing in wireless mesh networks," in *Proc. IEEE INFOCOM*, Apr. 2011, pp. 1907–1915.
- [117] Q. Lampin, D. Barthel, I. Auge-Blum, and F. Valois, "QoS oriented opportunistic routing protocol for wireless sensor networks," in *Proc. IFIP Wireless Days (WD)*, Nov. 2012, pp. 1–6.
- [118] Z. Wang, Y. Chen, and C. Li, "CORMAN: A novel cooperative opportunistic routing scheme in mobile ad hoc networks," *IEEE J. Sel. Areas Commun.*, vol. 30, no. 2, pp. 289–296, Feb. 2012.
- [119] S. Guo, L. He, Y. Gu, B. Jiang, and T. He, "Opportunistic flooding in low-duty-cycle wireless sensor networks with unreliable links," *IEEE Trans. Comput.*, vol. 63, no. 11, pp. 2787–2802, Nov. 2013.
- [120] M. Xiao, J. Wu, C. Liu, and L. Huang, "TOUR: Time-sensitive opportunistic utility-based routing in delay tolerant networks," in *Proc. IEEE INFOCOM*, Apr. 2013, pp. 2085–2091.
- [121] W.-Y. Shin, S.-Y. Chung, and Y. H. Lee, "Parallel opportunistic routing in wireless networks," *IEEE Trans. Inf. Theory*, vol. 59, no. 10, pp. 6290–6300, Oct. 2013.
- [122] X. Zhong, Y. Qin, Y. Yang, and L. Li, "CROR: Coding-aware opportunistic routing in multi-channel cognitive radio networks," in *Proc. IEEE Global Commun. Conf. (GLOBECOM)*, Dec. 2014, pp. 100–105.
- [123] M. Xiao, J. Wu, and L. Huang, "Community-aware opportunistic routing in mobile social networks," *IEEE Trans. Comput.*, vol. 63, no. 7, pp. 1682–1695, Jul. 2014.
- [124] C. Dong, L.-L. Yang, J. Zuo, S. X. Ng, and L. Hanzo, "Energy, delay, and outage analysis of a buffer-aided three-node network relying on opportunistic routing," *IEEE Trans. Commun.*, vol. 63, no. 3, pp. 667–682, Mar. 2015.
- [125] F. Wu, K. Gong, T. Zhang, G. Chen, and C. Qiao, "COMO: A game-theoretic approach for joint multirate opportunistic routing and forwarding in non-cooperative wireless networks," *IEEE Trans. Wireless Commun.*, vol. 14, no. 2, pp. 948–959, Feb. 2015.
- [126] M. Elias, A. Khattab, and K. M. F. Elsayed, "CORB: Context-aware opportunistic resource-based routing for stationary wireless sensor networks," in *Proc. Int. Conf. Comput., Netw., Commun. (ICNC)*, Feb. 2015, pp. 166–170.
- [127] K. Zeng, Z. Yang, and W. Lou, "Opportunistic routing in multi-radio multi-channel multi-hop wireless networks," *IEEE Trans. Wireless Commun.*, vol. 9, no. 11, pp. 3512–3521, Nov. 2010.
- [128] X. Zhang, A. Ghraryeb, and M. Hasna, "On hierarchical network coding versus opportunistic user selection for two-way relay channels with asymmetric data rates," *IEEE Trans. Commun.*, vol. 61, no. 7, pp. 2900–2910, Jul. 2013.
- [129] Y. Yan, B. Zhang, J. Zheng, and J. Ma, "CORE: A coding-aware opportunistic routing mechanism for wireless mesh networks," *IEEE Wireless Commun.*, vol. 17, no. 3, pp. 96–103, Jun. 2010.
- [130] A. M. Popescu, N. Salman, and A. H. Kemp, "Energy consumption analysis of geographic routing in WSNs with location error," in *Proc. 18th Eur. Wireless Conf., Eur. Wireless (EW)*, Apr. 2012, pp. 1–8.
- [131] Y. Li, Y. Jiang, D. Jin, L. Su, L. Zeng, and D. Wu, "Energy-efficient optimal opportunistic forwarding for delay-tolerant networks," *IEEE Trans. Veh. Technol.*, vol. 59, no. 9, pp. 4500–4512, Nov. 2010.
- [132] J. Zuo, C. Dong, S. X. Ng, L.-L. Yang, and L. Hanzo, "Cross-layer aided energy-efficient routing design for ad hoc networks," *IEEE Commun. Surveys Tuts.*, vol. 17, no. 3, pp. 1214–1238, Jan. 2015.
- [133] H. Ochiai, P. Mitran, and V. Tarokh, "Design and analysis of collaborative diversity protocols for wireless sensor networks," in *Proc. IEEE 60th Veh. Technol. Conf. (VTC-Fall)*, vol. 7, Sep. 2004, pp. 4645–4649.
- [134] A. Goldsmith, *Wireless Communication*, 1st ed. Cambridge, U.K.: Cambridge Univ. Press, 2005.
- [135] Q. Liu, S. Zhou, and G. B. Giannakis, "Cross-layer combining of adaptive modulation and coding with truncated ARQ over wireless links," *IEEE Trans. Wireless Commun.*, vol. 3, no. 5, pp. 1746–1755, Sep. 2004.
- [136] I. S. Gradshteyn and I. M. Ryzhik, *Table of Integrals, Series, and Products*, 7th ed. Amsterdam, The Netherlands: Elsevier, 2007.
- [137] *Meijer-G Function*. [Online]. Available: <http://functions.wolfram.com/>, accessed 1998–2015.
- [138] T. M. Cover and A. A. El Gamal, "Capacity theorems for the relay channel," *IEEE Trans. Inf. Theory*, vol. 25, no. 5, pp. 572–584, Sep. 1979.
- [139] A. Host-Madsen and J. Zhang, "Capacity bounds and power allocation for wireless relay channels," *IEEE Trans. Inf. Theory*, vol. 51, no. 6, pp. 2020–2040, Jun. 2005.
- [140] L. Kong, S. X. Ng, R. G. Maunder, and L. Hanzo, "Maximum-throughput irregular distributed space-time code for near-capacity cooperative communications," *IEEE Trans. Veh. Technol.*, vol. 59, no. 3, pp. 1511–1517, Mar. 2010.
- [141] M. F. U. Butt, R. A. Riaz, S. X. Ng, and L. Hanzo, "Distributed self-concatenated coding for cooperative communication," *IEEE Trans. Veh. Technol.*, vol. 59, no. 6, pp. 3097–3104, Jul. 2010.
- [142] S.-F. Chang and D. G. Messerschmitt, "Designing high-throughput VLC decoder. I. Concurrent VLSI architectures," *IEEE Trans. Circuits Syst. Video Technol.*, vol. 2, no. 2, pp. 187–196, Jun. 1992.

- [143] S. B. Korada and R. L. Urbanke, "Polar codes are optimal for lossy source coding," *IEEE Trans. Inf. Theory*, vol. 56, no. 4, pp. 1751–1768, Apr. 2010.
- [144] R. Y. Mesleh, H. Haas, S. Sinanović, C. W. Ahn, and S. Yun, "Spatial modulation," *IEEE Trans. Veh. Technol.*, vol. 57, no. 4, pp. 2228–2241, Jul. 2008.
- [145] I. Ahmed, A. Ikhlef, R. Schober, and R. K. Mallik, "Power allocation for conventional and buffer-aided link adaptive relaying systems with energy harvesting nodes," *IEEE Trans. Wireless Commun.*, vol. 13, no. 3, pp. 1182–1195, Mar. 2014.
- [146] N. Zlatanov and R. Schober, "Buffer-aided relaying with adaptive link selection—Fixed and mixed rate transmission," *IEEE Trans. Inf. Theory*, vol. 59, no. 5, pp. 2816–2840, May 2013.
- [147] N. Zlatanov, R. Schober, and P. Popovski, "Buffer-aided relaying with adaptive link selection," *IEEE J. Sel. Areas Commun.*, vol. 31, no. 8, pp. 1530–1542, Aug. 2013.



HUA SUN received the B.Eng. degree in electronics and information engineering from the Huazhong University of Science & Technology, Wuhan, China, in 2009, and the M.Sc. (Hons.) degree in wireless communications from the University of Southampton, Southampton, U.K., in 2010, where he is currently pursuing the Ph.D. degree with the Research Group of Communications, Signal Processing and Control, School of Electronics and Computer Science. His research

interests include superposition modulation, hierarchical modulation, turbo trellis-coded modulation, and cooperative communications.



CHEN DONG received the B.S. degree in electronic information sciences and technology from the University of Science and Technology of China, Hefei, China, in 2004, the M.Eng. degree in pattern recognition and automatic equipment from the University of Chinese Academy of Sciences, Beijing, China, in 2007, and the Ph.D. degree from the University of Southampton, U.K., in 2014. He currently holds a post-doctoral position with the University of Southampton. His research

interests include applied math, relay system, channel modeling, and cross-layer optimization. He was a recipient of a scholarship under the U.K.-China Scholarships for Excellence program. He received the best paper award at the IEEE VTC 2014-Fall.



SOON XIN NG (S'99–M'03–SM'08) received the B.Eng. (Hons.) degree in electronics engineering and the Ph.D. degree in wireless communications from the University of Southampton, Southampton, U.K., in 1999 and 2002, respectively. From 2003 to 2006, he was a Post-Doctoral Research Fellow working on collaborative European research projects known as SCOUT, NEWCOM, and PHOENIX. Since 2006, he has been a member of the Academic Staff with the

School of Electronics and Computer Science, University of Southampton. He is involved in the OPTIMIX and CONCERTO European projects and the IUATC and UC4G projects. He is an Associate Professor of Wireless Communications with the University of Southampton. He has authored over 180 papers and co-authored two John Wiley/IEEE Press books in his research field. His research interests include adaptive coded modulation, coded modulation, channel coding, space-time coding, joint source and channel coding, iterative detection, OFDM, MIMO, cooperative communications, distributed coding, quantum error correction codes, and joint wireless-and-optical-fiber communications. He is a Chartered Engineer and fellow of the Higher Education Academy, U.K.



LAJOS HANZO (F'90) received the degree in electronics in 1976, the Ph.D. degree in 1983, the Doctor Honoris Causa degree from the Technical University of Budapest, in 2009, and the D.Sc. degree. During his 38-year career in telecommunications, he has held various research and academic positions in Hungary, Germany, and U.K. Since 1986, he has been with the School of Electronics and Computer Science, University of Southampton, U.K., as the Chair in

Telecommunications. He has 23 000+ citations. He has successfully supervised 100 Ph.D. students, co-authored 20 *Mobile Radio Communications* (John Wiley/IEEE Press) books totaling in excess of 10 000 pages, authored over 1500 research entries at the IEEE Xplore, acted as the TPC Chair and General Chair of the IEEE conferences, presented keynote lectures, and received a number of distinctions. He is directing 60 strong academic research teams, working on a range of research projects in the field of wireless multimedia communications sponsored by the industry, the Engineering and Physical Sciences Research Council, U.K., the European Research Council's Advanced Fellow Grant, and the Royal Society's Wolfson Research Merit Award. He is an enthusiastic supporter of industrial and academic liaison. He offers a range of industrial courses. He is also a Governor of the IEEE VTS. From 2008 to 2012, he was the Editor-in-Chief of the *IEEE Press* and a Chaired Professor with Tsinghua University, Beijing. His research is funded by the European Research Council's Senior Research Fellow Grant. He is a fellow of REng, IET, and EURASIP.

• • •